



5-2022

VALIDATION OF RELAP5-3D FOR TRANSIENT SIMULATION OF LEAD-LITHIUM SYSTEMS FOR FUSION APPLICATIONS

Nicholas Akira Meehan
nmeehan@vols.utk.edu

Follow this and additional works at: https://trace.tennessee.edu/utk_gradthes



Part of the [Nuclear Engineering Commons](#)

Recommended Citation

Meehan, Nicholas Akira, "VALIDATION OF RELAP5-3D FOR TRANSIENT SIMULATION OF LEAD-LITHIUM SYSTEMS FOR FUSION APPLICATIONS. " Master's Thesis, University of Tennessee, 2022.
https://trace.tennessee.edu/utk_gradthes/6422

This Thesis is brought to you for free and open access by the Graduate School at TRACE: Tennessee Research and Creative Exchange. It has been accepted for inclusion in Masters Theses by an authorized administrator of TRACE: Tennessee Research and Creative Exchange. For more information, please contact trace@utk.edu.

To the Graduate Council:

I am submitting herewith a thesis written by Nicholas Akira Meehan entitled "VALIDATION OF RELAP5-3D FOR TRANSIENT SIMULATION OF LEAD-LITHIUM SYSTEMS FOR FUSION APPLICATIONS." I have examined the final electronic copy of this thesis for form and content and recommend that it be accepted in partial fulfillment of the requirements for the degree of Master of Science, with a major in Nuclear Engineering.

Nicholas R. Brown, Major Professor

We have read this thesis and recommend its acceptance:

Nicholas R. Brown, G. Ivan Madlonado, David C. Donovan

Accepted for the Council:

Dixie L. Thompson

Vice Provost and Dean of the Graduate School

(Original signatures are on file with official student records.)

**VALIDATION OF RELAP5-3D FOR
TRANSIENT SIMULATION OF LEAD-LITHIUM
SYSTEMS FOR FUSION APPLICATIONS**

A Thesis Presented for the
Master of Science
Degree
The University of Tennessee, Knoxville

Nicholas Akira Meehan
May 2022

Copyright © 2022 by Nicholas Akira Meehan
All rights reserved.

ACKNOWLEDGEMENTS

The author would like to thank Dr. Nicholas R. Brown for providing him with this incredible opportunity and for guidance and encouragement which helped him to succeed throughout graduate school. The author would like to thank Dr. Seokbin Seo for help in developing the RELAP5-3D models and for providing guidance in the project. The author would like to thank Felipe Novais for help in developing the MCNP model, and Kenneth Bott for help in performing calculations using the MCNP model. The author would also like to thank Mr. Robert Kile and Mr. Edward Duchnowski for their guidance in progressing through my graduate studies as both friends and mentors. The author would like to thank his family for their unwavering support in his ambitions.

The author acknowledges the support from the US Department of Energy, Office of Fusion Energy Sciences under contract No. DE-AC05-00OR22725.

ABSTRACT

With increasing development in fusion technology including the construction and subsequently planned experimental campaign of the International Thermonuclear Experimental Reactor (ITER), validation must be performed for simulation tools used in the design, development, and licensing of future commercial fusion systems. This thesis contains several validation studies for transient simulation of lead-lithium eutectic (PbLi) systems using the RELAP5-3D code. This validation analysis is performed initially using models of systems without the influence of a magnetic field to inspect heat transfer and pressure drop phenomena. The validation study then uses models of systems under the influence of a magnetic field to inspect magnetohydrodynamic (MHD) pressure drop phenomena. We determine that the results from the validation study show excellent agreement to experimental results and that RELAP5-3D is sufficient for modeling PbLi systems for fusion relevant applications.

This following work constructs a model of the Dual-Coolant Lead-Lithium (DCLL) blanket design from the proposed Fusion Nuclear Science Facility (FNSF). This is used to perform a representative startup transient of the FNSF based on limitations of both light water reactors and PbLi tandem mirror systems. This model provides a baseline for thermal-hydraulic analysis of PbLi blanket systems. Suggestions for further improvement of the model are given including the implementation of a multiphysics analysis, the enhancement of the MHD calculation capabilities, and the development of a simple thermomechanical analysis.

TABLE OF CONTENTS

| | |
|--|----|
| Chapter One Introduction..... | 1 |
| The Fusion Nuclear Science Facility..... | 1 |
| Modeling and Simulation Tools..... | 3 |
| RELAP5-3D and Potential Application to Fusion Analysis..... | 4 |
| Chapter Two Literature Review | 6 |
| MHD Interaction Characteristics | 6 |
| Previous Fusion Blanket Analysis Using ROMs..... | 10 |
| Experimental MHD Test Facilities..... | 10 |
| ALEX Experimental Campaign and MHD Studies | 10 |
| Previous MaPLE MHD Studies | 13 |
| Previous DCLL Studies..... | 15 |
| LWR AOOs and DBAs for Fusion | 16 |
| Startup Transients | 17 |
| Chapter Three Validation Basis for RELAP5-3D..... | 22 |
| Representative Flow Loop..... | 22 |
| Background and Methods | 22 |
| Results..... | 22 |
| Natural Circulation Loop (ORNL)..... | 25 |
| Background and Methods..... | 25 |
| Results..... | 30 |
| ALEX Facility (ANL)..... | 30 |
| Background and Methods..... | 30 |
| Results..... | 37 |
| MaPLE Loop (UCLA)..... | 37 |
| Background and Methods..... | 37 |
| Results..... | 40 |
| Conclusions | 47 |
| Chapter Four DCLL Model For Thermal-Hydraulic Analysis | 48 |
| Model Development and Specifications | 48 |
| Startup Transient Results | 52 |
| Chapter Five Conclusions and Recommendations | 57 |
| List of References | 64 |
| Vita..... | 72 |

LIST OF TABLES

| | |
|--|----|
| Table 3.1. Representative Flow Loop Operational Conditions | 26 |
| Table 3.2. Natural Circulation Loop Model Specifications..... | 29 |
| Table 3.3. Natural Circulation Loop Steady State Flow Parameters | 33 |
| Table 3.4. ALEX Facility MHD Parameters | 36 |
| Table 3.5. MaPLE Loop MHD Parameters..... | 42 |
| Table 3.6. MaPLE Loop Change in MHD Pressure Vs Change in Flow Rate | 45 |
| Table 3.7. RELAP5-3D Error in MHD Pressure Drop Magnitude..... | 45 |
| Table 3.8. RELAP5-3D Error in Change in MHD Pressure Drop vs Change in Flow Rate..... | 46 |
| Table 4.1. DCLL Model Operational and MHD Parameters. | 51 |
| Table 5.1. DCLL Blanket Outlet Temperature with Helium Coupling | 63 |

LIST OF FIGURES

| | |
|--|----|
| Figure 1.1. DCLL Blanket Compared to Alternate Blanket Designs [5] | 2 |
| Figure 2.1. MHD Flow Force Diagram Within a Conducting Pipe | 7 |
| Figure 2.2. MHD Flow Force Diagram With Velocity Profile Overlaid | 7 |
| Figure 2.3. MHD Flow Force Diagram With Perfectly Insulating FCI | 9 |
| Figure 2.4. ALEX MHD Benchmark Data (Rectangular Channel) | 12 |
| Figure 2.5. ALEX MHD Benchmark Data (Circular Channel) | 12 |
| Figure 2.6. MaPLE MHD Benchmark Data (Circular Channel) [46] | 14 |
| Figure 2.7. Normalized Tore Supra Power Pulse Based on Experimental Campaign [70] | 20 |
| Figure 2.8. Representative Normalized Startup Transient Based on Thermal Stress Limitations | 21 |
| Figure 3.1. Representative Flow Loop Nodalization..... | 23 |
| Figure 3.2. Representative Flow Loop Transient Temperature Difference Across Hot Leg | 24 |
| Figure 3.3. Representative Flow Loop Transient Average Heat Flux Across Hot Leg..... | 26 |
| Figure 3.4. Natural Circulation Loop Design | 27 |
| Figure 3.5. Natural Circulation Loop Nodalization Diagram | 28 |
| Figure 3.6. Forms Loss Coefficient Curve Fit Using Parametric Data [75]..... | 31 |
| Figure 3.7. Natural Circulation Loop Null Transient Temperature Distribution | 32 |
| Figure 3.8. Natural Circulation Loop Null Transient Flow Velocity | 32 |
| Figure 3.9. ALEX Facility Loop Design | 35 |
| Figure 3.10. ALEX Facility Nodalization Diagram | 35 |
| Figure 3.11. ALEX Facility Pressure Distribution Relative to Inlet Pressure | 38 |
| Figure 3.12. ALEX Facility Dimensionless Pressure Drop for Circular Channel Geometry | 39 |
| Figure 3.13. MaPLE Loop Design | 41 |
| Figure 3.14. MaPLE Loop Nodalization Diagram | 41 |
| Figure 3.15. MHD Pressure Drop Across Uniform Field Test Section using RELAP5-3D Properties | 43 |
| Figure 3.16. MHD Pressure Drop Across Uniform Field Test Section Using Literature Review Properties from [74] | 44 |
| Figure 4.1. FNSF Inboard Blanket Sector Cross Section [7] | 49 |
| Figure 4.2. DCLL Model Nodalization Diagram..... | 50 |
| Figure 4.3. Representative DCLL Channel Cross Section | 51 |
| Figure 4.4. DCLL Radial Power Density Distribution..... | 53 |
| Figure 4.5. DCLL Normalized Representative Startup Transient | 55 |
| Figure 4.6. DCLL Transient Outlet Temperature..... | 56 |
| Figure 5.1. MCNP CAD Model Diagram of the FNSF (Left) and of One Sector (Right)..... | 59 |

Figure 5.2. MCNP Calculated Radial Heating Profiles for the Inboard Blanket
(Left) and Outboard Blanket (Right).....59

Figure 5.3. RELAP5-3D DCLL Blanket Helium Channel Coupling Diagram60

Figure 5.4. DCLL Transient PbLi Outlet Temperature.....62

Figure 5.5. DCLL Transient Helium Outlet Temperature.....62

CHAPTER ONE

INTRODUCTION

Nuclear fusion is a field that has incredible potential for the future of the energy industry. Having been in development since the early 1950's, we are fast approaching the inception of the first commercial fusion power plant. Of the two main approaches to confine fusion plasma, significant development has been made towards making magnetic confinement fusion possible using tokamak style reactors [1]. Most recently, the construction and planned experimental campaign of the International Thermonuclear Experimental Reactor (ITER) plans to incorporate advanced tokamak components such as superconducting magnets and operate at long-term high-temperature conditions representative of a commercial power plant [1]. Designs have thus been proposed for a potential DEMOnstration commercial reactor (DEMO) but, with potentially large technological gaps between the technology of ITER and DEMO, an intermediate facility may be necessary [2]. The United States (US) have proposed a design for such a facility, the Fusion Nuclear Science Facility (FNSF) with the goal of facilitating the transition to DEMO through addressing materials and thermal limits for the blanket and divertor components [2].

The Fusion Nuclear Science Facility

The FNSF is a proposed fusion tokamak system designed to operate at temperatures representative of a potential commercial fusion power plant [2]. The FNSF design includes the US-based dual coolant lead-lithium (DCLL) blanket design for heat extraction and tritium production [2]. The DCLL blanket uses two different coolants; helium to cool the structural material and liquid PbLi as a target for tritium breeding and to remove volumetric heat generated within the blanket [2]. The DCLL blanket is a primary candidate for use in US commercial fusion plants since the liquid PbLi offers high thermal efficiency compared to alternative helium cooled blankets that utilize reduced activation ferritic/martensitic (RAFM) steel structural material and PbLi breeder [3]. Some of the main concerns for this blanket design are the interaction between the strong magnetic field and the flowing PbLi causing magnetohydrodynamic (MHD) effects, and the compatibility of the high temperature PbLi with the temperature limits of the RAFM steel structural material [3]. These issues are addressed with the development of a flow channel insert (FCI) made of a non-conductive material with a high melt temperature such as silicon carbide (SiC) [4]. The FCI is placed within the channel and insulates the PbLi both thermally and electrically, mitigating the MHD pressure drop from interaction with the magnetic field and keeping the structural RAFM steel from exceeding temperature limits. Further details regarding the advantages and disadvantages of the DCLL blanket compared to alternative PbLi blanket designs are highlighted in Figure 1.1.

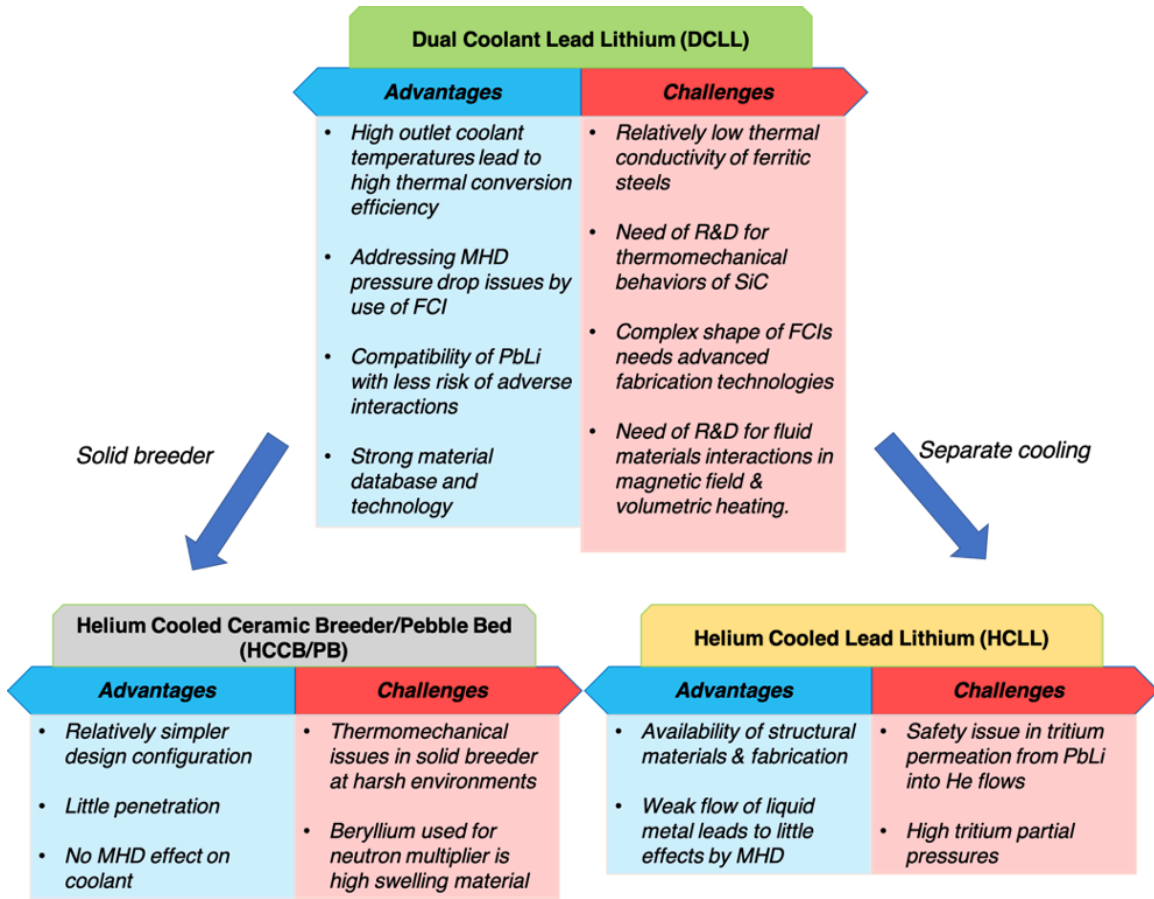


Figure 1.1. DCLL Blanket Compared to Alternate Blanket Designs [5]

Research and development for the licensing of fusion facilities such as the proposed Fusion Nuclear Science Facility (FNSF) requires the use of experiments and computational models that can capture the multiphysics interactions within the blanket region [6]. Separate effects tests of the Dual Coolant Lead Lithium (DCLL) blanket concept, the proposed blanket design for the FNSF, including thermo-mechanical stress [7], MHD pressure drop and flow distribution [4, 8], and neutronics [9], have been investigated in the past using high fidelity 3-D codes. The use of high fidelity modeling techniques is beneficial for understanding the phenomena within separate effects tests since they include spatial discretization. However, the computational time and power necessary for high fidelity models is impractical for use in systems-level iterative multiphysics calculations which are essential for developing transient safety analyses for a highly coupled system such as the blanket. To address this, a research project initiated to construct a multiphysics framework for transient blanket analysis using reduced order models (ROMs). This framework would include coupled models for neutronics, thermal-hydraulics and tritium transport aspects of the DCLL blanket. RELAP5-3D has been selected to perform the thermal-hydraulic analysis within the multiphysics framework since it is a well-established thermal-hydraulic simulation tool for the safety analysis of LWR systems that is capable of handling multiple working fluids and utilizing ROM's [10].

Modeling and Simulation Tools

To perform the safety analysis of the system, transient analysis of all potential operational scenarios must be performed. This requires the calculation of key system parameters such as temperatures, pressures, radiation damage, and stresses. To accomplish this, models are created focusing on specific aspects of the reactor system such as thermal-hydraulics, neutronics, and thermomechanical interactions. These phenomena are analyzed using simulation tools of varying fidelity. Typically, as fidelity of the simulation model increases, the analysis is limited to a component level to account for the increase in required computational power. This means that while higher fidelity models are capable of in-depth analysis of a single component, there is no way to capture the interaction between the component and the rest of the system. Lower fidelity systems level models are not able to fully resolve the local phenomena, however since they require less computational power and time, they are capable of analyzing the system response as a whole. This shows a distinct need for both component and system level simulations using models of both high and low fidelity, respectively. This ensures both local and average values of key parameters do not exceed design constraints and appropriate level of fidelity for the analysis can be determined.

Tools commonly used for transient thermal-hydraulics analysis for fusion systems include system level codes such as RELAP [11, 12], MELCOR [13-15], component level codes including STAR-CCM+ [16], ANSYS [4, 17-20],

GETTHEM [21-23] and independently developed numerical modeling codes [24]. For high fidelity component level calculations, finite element codes such as ANSYS, STAR-CCM+ and numerical codes are traditionally used. Several studies of the DCLL blanket utilizing such component level code capabilities included spatial distribution of temperatures and thermal stresses [7], and flow velocity under MHD conditions [8]. This allowed for the inspection of local maximums and gradients within their models, however the model was limited to the blanket region. Lower fidelity system level calculations are typically performed using codes such as MELCOR and RELAP5-3D, which can both utilize ROMs. Previous fusion blanket studies have shown similar simulation capability between RELAP and MELCOR with the only advantage being user preference [25-29]. Unlike the component level simulations, the MELCOR and RELAP models included the blanket and the full primary and secondary coolant loops across several accident transients. These models would need to be tuned to capture specific localized effects such as MHD interactions, but would still have a lower computational load. This offers a distinct advantage over component level models since the scope of the simulation encompasses the surrounding systems coupled to the component of interest and can provide transient feedback through plant control responses. It is for this reason that we will be using a systems level code for the multiphysics analysis of the DCLL blanket.

RELAP5-3D and Potential Application to Fusion Analysis

The RELAP5-3D code is a version of the RELAP code developed for the Department of Energy (DOE) with a shared validation basis for licensing of light water reactors [10]. RELAP5-3D has previously been determined to be in accord with NQA-1 2008/2009a, DOE and EPRI technical reports guidance; nuclear code quality assurance for use in nuclear facility safety functions [30]. This gives the code an advantage over independently developed numerical codes when being considered for standard use in safety analysis for fusion systems since it has an established safety analysis background.

RELAP5-3D calculates transient values by solving the mass, momentum, and energy equations semi-implicitly in time, and utilizes finite difference approximations in space [31]. This simplifies the system of differential equations used for hydrodynamic analysis to allow for rapid transient calculation of system parameters. By using RELAP5-3D, we will be able to take advantage of ROMs which will provide fast, accurate transient thermal-hydraulic analysis within the iterative multiphysics framework. The RELAP5-3D code has recently expanded its capabilities to include numerous working fluids including lead-lithium eutectic (PbLi), which have not been previously validated [31, 32]. RELAP5-3D is also capable of simulating multiple working fluids within a single model, unlike the MELCOR code which is only capable of one working fluid in place of the default

water coolant [33]. This will be essential for the modeling of the DCLL blanket design which requires both helium and PbLi.

This thesis aims to develop a model within RELAP5-3D for transient thermal-hydraulic analysis of the DCLL blanket. This will be done using several goals working toward the overall objective

1. Perform a literature review of previous experimental PbLi systems and DCLL blanket design for experimental validation of the RELAP5-3D code
2. Develop a validation basis and modeling methodology for the analysis of PbLi systems under fusion relevant conditions using the RELAP5-3D code
 - Perform experimental validation of heat transfer and pressure drop within PbLi systems
 - Perform experimental validation of magnetohydrodynamic pressure drop due to the influence of a magnetic field
3. Use the modeling methodology and validation basis to construct a model of the DCLL blanket for transient analysis within RELAP5-3D.
 - Perform validation of the DCLL blanket model using design parameters from literature

CHAPTER TWO

LITERATURE REVIEW

In developing a validation basis for PbLi simulation within RELAP5-3D, a review of experimental and computational analyses of selected PbLi systems was conducted. This will assist in determining potential methods and experimental data for analyzing PbLi systems using ROMs. Within this study we will be inspecting systems with the influence of a magnetic field. Systems under the influence of a magnetic field are of particular interest since MHD interaction is a major limiting factor of the DCLL blanket design. Understanding the MHD interactions within flow channels can better inform us of potential changes in heat transfer and pressure effects and how to account for them in the DCLL model.

The demonstration of safe operation over all anticipated operational occurrences (AOOs) and design basis accidents (DBAs) is necessary for licensing systems that do not have a long-standing operational history as stated within NUREG-1537 [34]. To facilitate this, a review of light water reactor (LWR) AOOs and DBAs that are considered for licensing is conducted. From this review, we can determine the scope for the DCLL analysis and the most appropriate transient to use when designing and testing our model.

MHD Interaction Characteristics

Within the FNSF design, strong magnetic fields exist in the toroidal and poloidal direction with a planned peak field strength exceeding 5T in the blanket region [35]. The flowing liquid metal PbLi within the DCLL blanket will undergo MHD interactions effecting heat transfer and pressure gradients within the channel while under the influence of the magnetic field. MHD interactions begin when the flowing PbLi interacts with the magnetic field of the system and causes the formation of electrical eddy current loops. When these current loops close within the conducting channel boundary material, in this case RAFM steel, the field lines are limited to flowing in one direction within the bulk flow. The interaction between the magnetic and electric field lines produces a force known as the Lorentz force which, in this case, opposes the bulk flow. This concentrates the bulk flow toward the non-conducting side walls of the channel, parallel to the magnetic field. The flow distribution forms an MHD flow profile, known as Hunt flow, which consists of low velocity flow in the center of the channel and high velocity jets near the non-conducting walls parallel to the magnetic field [36]. The MHD interaction force diagram within a rectangular conducting channel can be seen in Figure 2.1, and the same diagram with a representative velocity profile can be seen in Figure 2.2.

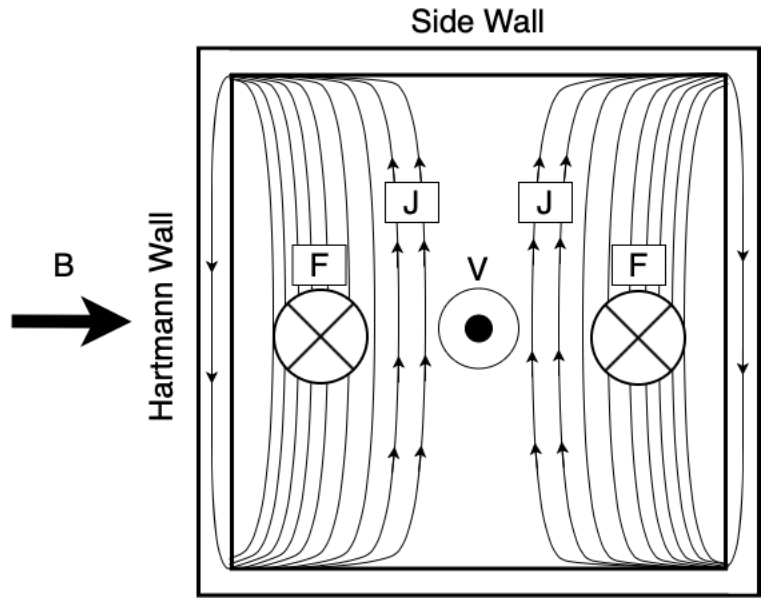


Figure 2.1. MHD Flow Force Diagram Within a Conducting Pipe

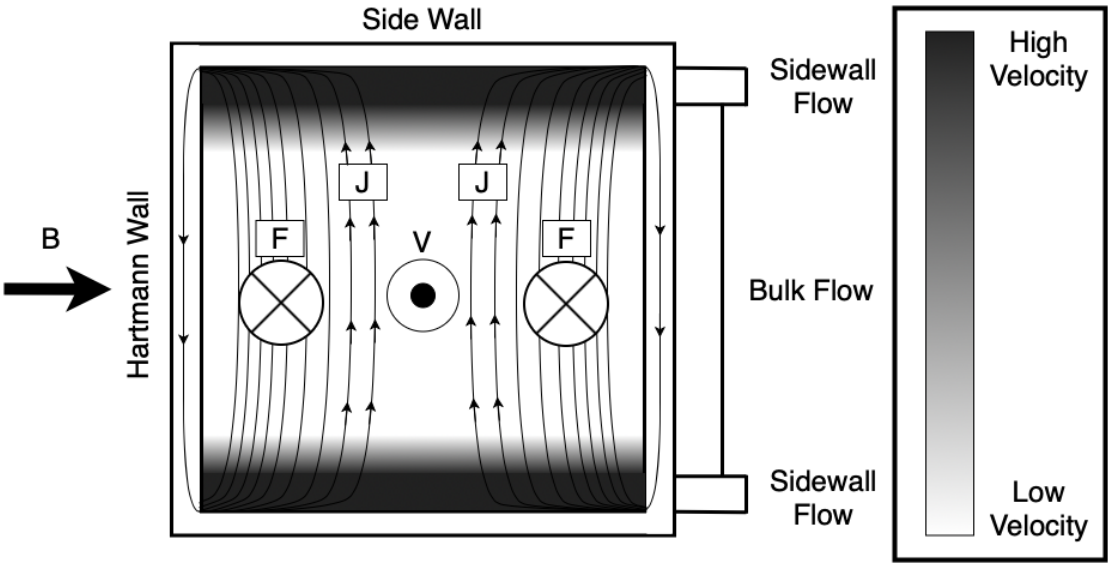


Figure 2.2. MHD Flow Force Diagram With Velocity Profile Overlaid

Within these diagrams, the magnetic field is represented by B, the velocity of the PbLi is represented by V, the eddy currents are represented by J and the Lorentz force is represented by F.

These velocity jets will affect the heat transfer across the side walls, but the major drawback, and ultimately limiting factor, is the consequent pressure drop which must be accounted for using pumps [8]. Ideally, within a perfectly insulating boundary, the eddy current loops would be able to close within the bulk flow, causing the Lorentz Force to cancel itself out, and providing a fully-developed flow profile without the influence of thermal gradient effects. Current DCLL designs reduce the MHD interaction force by thermally and electrically insulating the channel with an FCI, however it is still a major design constraint for the DCLL design even when the effects are mitigated [4, 8, 37-40]. A sample channel force diagram representing a perfectly insulating FCI is shown in Figure 2.3.

Important dimensionless values regarding MHD flow are the Hartmann number, Reynolds number, the Interaction parameter. The Hartmann number is the ratio between the electromagnetic and viscous forces, the Reynolds number is the ratio between internal and viscous forces, and the Interaction parameter is the ratio between the electromagnetic forces to inertial forces. These parameters are defined in equations 1-3, and related by equation 4.

$$Ha = BL \sqrt{\frac{\sigma}{\mu}} \quad (1)$$

$$Re = \left[\frac{\rho v L}{\mu} \right] \quad (2)$$

$$N = \left[\frac{\sigma L B^2}{\rho v} \right] \quad (3)$$

$$N = \left[\frac{Ha^2}{Re} \right] \quad (4)$$

At high Hartmann numbers and high Interaction parameters, which are characteristic of liquid metal flow within fusion blanket systems, the flow can be defined in separate regions based on the boundary layers of the flow [41]. Two pairs of boundary layers exist, the Hartmann and Shercliff layers. The Hartmann layers are adjacent to the Hartmann walls and the Shercliff layers are adjacent to the non-conducting walls parallel to the magnetic field. Heat transfer characteristics of the flow are heavily dependent on the Hartmann number and subsequent development of the flow boundary layers. A strong magnetic field increases the stability of the flow, which requires a higher Reynolds number to initiate the transition to turbulent flow.

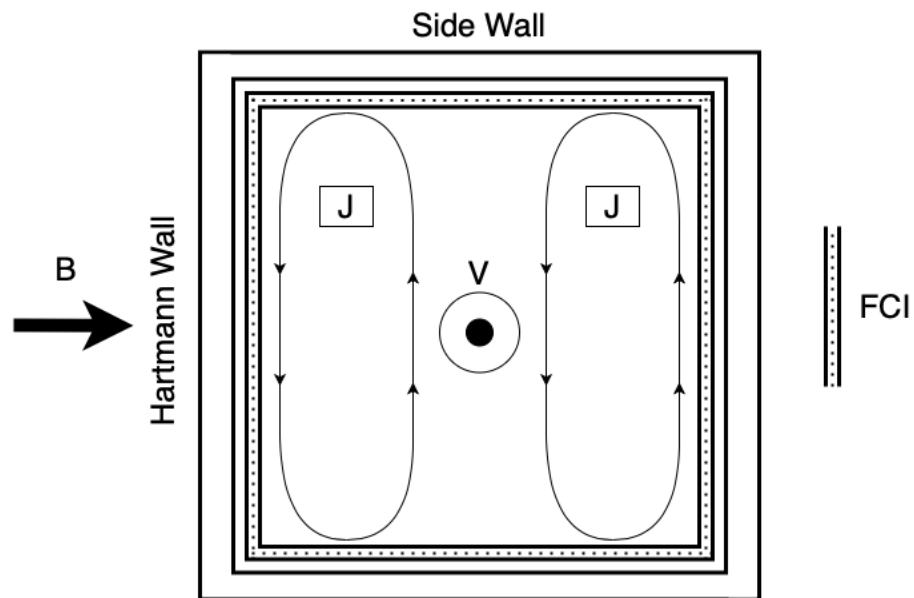


Figure 2.3. MHD Flow Force Diagram With Perfectly Insulating FCI

This means that under a stronger magnetic field, the heat transfer within the PbLi will be significantly less than a flow under a lower strength magnetic field with same Reynolds number. This effect should be accounted for within the model but may not be necessary if the Hartmann number and Interaction parameter can be lowered with the use of an FCI.

Previous Fusion Blanket Analysis Using ROMs

ROMs such as those built within the RELAP5-3D code have previously been used for accident analysis of several breeder concepts including the European Helium-Cooled Lead-Lithium (HCLL) and Helium-Cooled Pebble Bed (HCPB) designs [26-29]. Of particular interest between these is the HCLL design which utilizes flowing liquid PbLi solely for breeding tritium and is fully cooled by pressurized helium unlike the DCLL design which uses PbLi as an additional coolant [42]. While these studies successfully analyzed liquid PbLi systems using RELAP5-3D ROMs, they deemed the MHD effect within the blanket to be of low importance and ignored it. Since the flowrate of PbLi within the HCLL design is much slower than that of the DCLL design, the Lorentz force decreases and the overall impact of the MHD effects are negligible [26]. However, this motivates the need for the validation of MHD effects within RELAP5-3D ROMs for the analysis of the DCLL blanket design.

Experimental MHD Test Facilities

Several experimental test facilities, namely the Argonne Liquid metal EXperiment (ALEX) facility and Magnetohydrodynamic PbLi Experiment (MaPLE) facility, were constructed to investigate the pressure effects and flow distribution changes due to MHD flow conditions [43, 44]. As previously mentioned, high fidelity 3-D numerical solvers have been developed to inspect 3-D MHD flow effects which have been validated using experimental data from the ALEX and MaPLE facilities respectively [45-47]. Experimental data from these same facilities will serve as a benchmark for the validation of RELAP5-3D ROMs to ensure they capture the same phenomena demonstrated by high fidelity simulations.

ALEX Experimental Campaign and MHD Studies

The ALEX facility experimental campaign has been used for several international MHD benchmark cases including the pressure drop across a non-uniform transverse magnetic field following a uniform field region using both cylindrical and rectangular channel geometry [48]. The original benchmark study inspected the 3-D pressure gradient across the fringing field and the transverse pressure difference between the flows across the Hartmann walls, perpendicular to the magnetic field, and of the non-conducting walls parallel to the magnetic field, and the velocity profile through a fringing field [49]. As expected, the flow formed the aforementioned typical Hart flow velocity profile and the MHD interaction within the channel caused a pressure differential between the Hartmann wall flows and

the non-conducting side wall flow. The dimensionless pressure drop benchmark cases have been used to validate 3-D MHD simulation codes, namely OpenFOAM, COMSOL, HIMAG, and other numerical solvers, which all showed good agreement across both the circular and rectangular geometry [50-53]. Additionally, code validation was done for the ATHENA code using these benchmark cases using ROMs which also showed good agreement to both cases [54, 55].

The two benchmark validation cases are shown in Figures 2.4 and 2.5 which are plotted against results from high fidelity 3-D MHD codes. The round channel had an interaction parameter, N , of 10700, and a Hartmann number, M , of 6600, and the rectangular channel had an interaction parameter and Hartmann number of 540, and 2900, respectively. The units on the Y axis are a dimensionless parameter for expressing the pressure drop, ΔP , over a length of the channel, ΔX , using the fluid electrical conductivity, σ , the average channel velocity, U , and the magnetic field strength, B . The units on the X axis are the distance from the outlet of the uniform magnetic field region, x , made dimensionless using the channel half-width, L . The outlet of the uniform magnetic field region is at 0 such that the uniform magnetic region is the section is to the left and the region outside the magnetic field is to the right. From this, we observe that as the flow leaves the magnetic field region, the MHD pressure drop gradually decreases due to the decrease in magnetic field strength. We can also observe that the pressure drop is stronger for the case within the rectangular channel.

The ALEX facility was later converted from a sodium-potassium eutectic (NaK) loop operating at room temperature to a Vanadium/Lithium system operating at 350C to support the ITER blanket development program [56, 57]. Experiments following this change focused on inspecting the mitigation of the MHD effect using inner wall coatings to electrically insulate the channel. The benchmark cases with NaK were repeated with such an insulating coating prior to the upgrade and found that the insulating channel coating reduced the MHD pressure effects in the transverse direction [58]. These experiments are the predecessor to the eventual development of the FCI which is currently used in blanket design for MHD mitigation in the DCLL blanket [4, 42].

This gives us an understanding of the extensive background in experimental MHD code validation from the ALEX facility experimental campaign. With this in mind, the ALEX facility serves as an excellent validation source for our MHD implementation in RELAP5-3D. For our validation, we will be using the benchmark cases used to validate the ROMs developed in the ATHENA code [55]. We will be using an implementation of the MHD effects similar to this study by applying an equivalent wall friction factor to the channel.

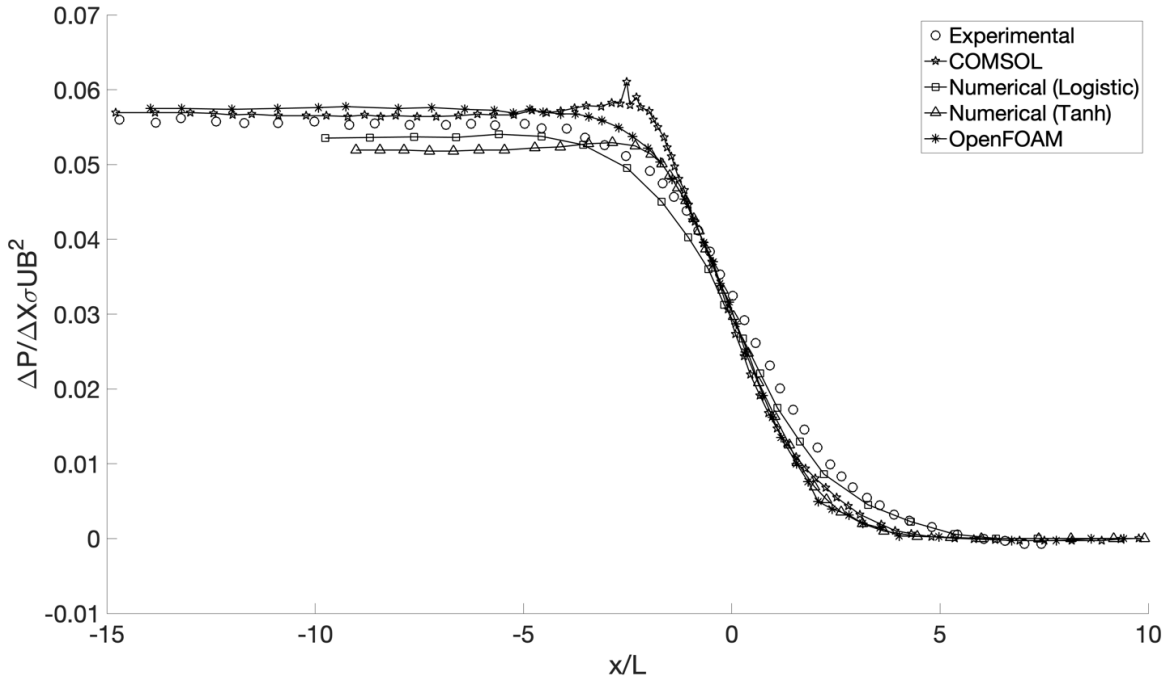


Figure 2.4. ALEX MHD Benchmark Data (Rectangular Channel)

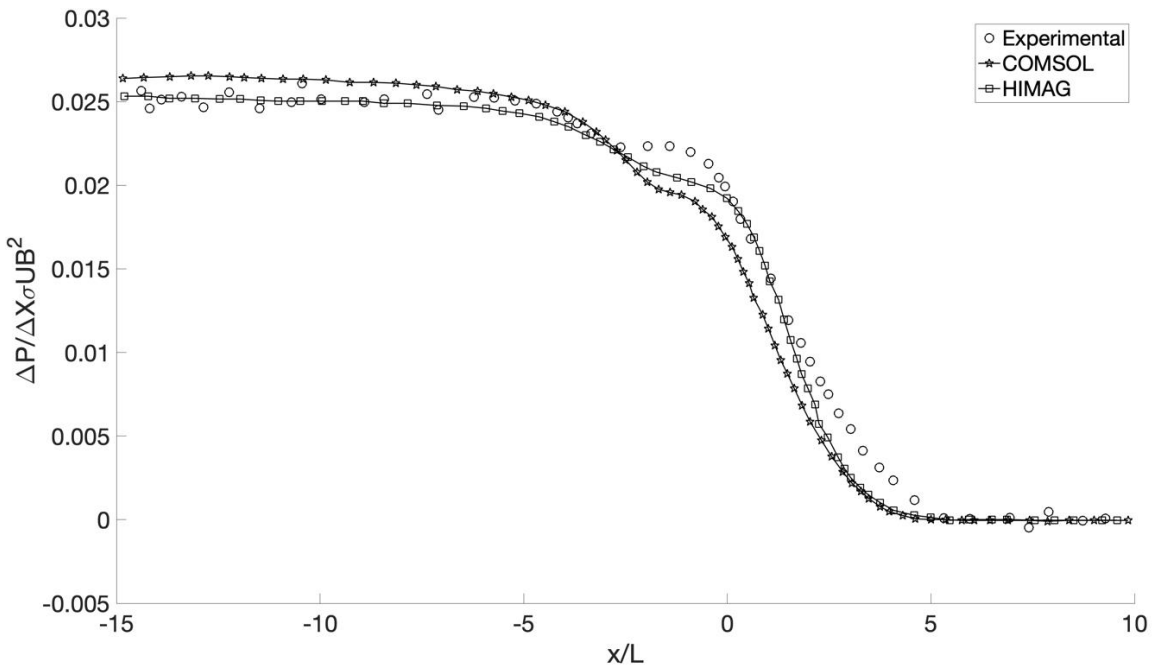


Figure 2.5. ALEX MHD Benchmark Data (Circular Channel)

Previous MaPLE MHD Studies

MHD experiments within the MaPLE loop have been designed to inspect the implementation of FCIs within the flow channels for supporting the development of the US based DCLL blanket design [59]. One experiment performed was the performance analysis of a foam SiC FCI looking at both the material interaction with the FCI and the impact in reducing the MHD pressure drop [47]. This FCI proved to be insufficiently compatible with the PbLi as there was large ingresses in the FCI, degrading the performance. However, the initial experimental MHD pressure drop data was taken with a bare duct at varying flowrates under a constant magnetic field of 1T. This data agreed well with a numerical analysis using a MHD correlation for fully developed flow within an electrically conducting pipe with thin walls, and can provide us with experimental pressure drops for verification of our RELAP5-3D implementation of MHD pressure drop [59].

Further MHD experimentation was performed within the MaPLE loop specifically inspecting fringing field phenomena [46]. The experiments were performed in a conducting circular channel with a uniform region of 1T. Pressure drop measurements were taken for the flow entering and leaving the uniform magnetic field at either end of the test section. The test conditions are similar to the international benchmark problem of the ALEX facility, which is one of several experiments for MHD code validation [48]. Data from this MaPLE experiment were also used to validate the HIMAG code, a 3-d numerical code for MHD flow simulation [60]. The data was also compared to a uniform MHD pressure drop correlation for circular channels developed by Miyazaki et. al. which is given by Equation 5 [61].

$$\Delta p = L \frac{c_w}{1+c_w} \sigma_f U B_0^2 \quad (5)$$

Within this equation, L is the distance travelled within the channel, σ_f is the fluid electrical conductivity, U is the average flow velocity, and B_0 is the magnetic field strength. The term c_w is ratio of the wall electrical conductivity to the fluid electrical conductivity multiplied by the ratio of the wall thickness to the channel half-width. This is given by Equation 6 where σ_w is the wall electrical conductivity, r_i is the inner radius of the channel, also known as the channel half width, and r_o is the outer radius of the channel.

$$c_w = \frac{\sigma_w(r_o-r_i)}{\sigma_f \cdot r_i} \quad (6)$$

Three pairs of measurements were made with each pair having the same Hartmann number and different Reynolds numbers. The comparison between the experimental, simulation, and equation values are shown in Figure 2.6.

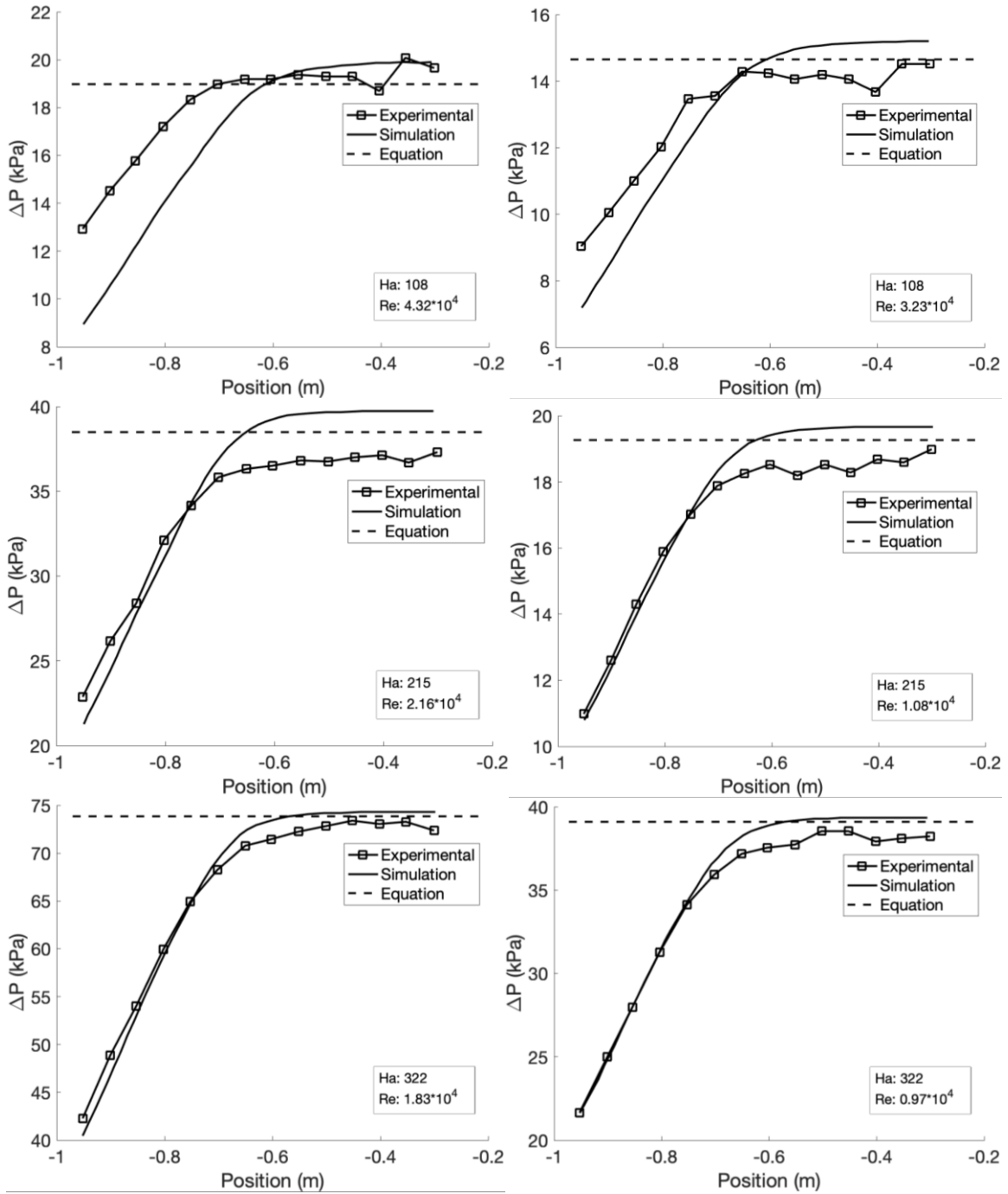


Figure 2.6. MaPLE MHD Benchmark Data (Circular Channel) [46]

The data shown shows very similar trends to that of the ALEX benchmark data in terms of the shape of the pressure drop curve and of the MHD review which shows that pressure drop increases with both increasing Hartmann number and increasing Reynolds number.

The initial MHD experimental campaign following the initial construction of the loop focused on verifying the accuracy of the pressure drop measurement systems across the uniform magnetic field section within the loop [44]. To accomplish this, measured data at various magnetic field strengths and flowrates were compared against theoretical values. The theoretical values were calculated using an equation with good accuracy for NaK flow under fully developed flow conditions within thick, electrically conductive walls [61] and showed good agreement over all the experimental cases. The experimental data from this initial operation has incredible potential for the validation of our MHD implementation in RELAP5-3D since the data covers a wide variety of flow conditions and magnetic field strengths and is under the influence of a uniform magnetic field. We can also use our determined uniform magnetic field pressure drop and compare the results to the correlation from equation 5.

Previous DCLL Studies

As discussed in Section 1, the DCLL blanket design requires an in-depth multiphysics analysis to capture the complex interactions within the system. A sample multiphysics feedback mechanism would be as follows [6]:

- 1) The flow distribution of within the PbLi channels is determined by the MHD interactions within the channel and volumetric nuclear heating
- 2) The resulting temperature gradients cause thermal stresses which are applied to the FCI
- 3) Irradiation within the channel and thermal stresses cause the FCI's insulating properties to degrade
- 4) The MHD interactions are changed due to the change in properties of the FCI

Separate effects tests of the Dual Coolant Lead Lithium (DCLL) blanket concept, the proposed blanket design for the FNSF, including thermo-mechanical stress [7, 17], MHD pressure drop and flow distribution [4, 8, 20, 37, 47, 62], and neutronics [9], have been investigated in the past using high fidelity 3-D codes. Of these effects, the main focuses for this study are the MHD pressure drop, temperature, flow distribution models. However, since we are unable to determine the velocity profiles within the flow using a 1-D ROM analysis, we will focus on the temperature and pressure drop to determine a benchmark for the validation of our DCLL model. The most complete studies based on the criteria of our benchmark study are those performed by Smolentsev et. al. [8], and Huang et. al. [7].

Within the first study performed by Smolentsev et. al., a numerical analysis is performed on the DCLL channel calculating the MHD pressure drop with and without the influence of a SiC FCI. This includes each component of the blanket system including the inlet and outlet manifolds, the access pipes, redistribution section and, most importantly, the poloidal channel flow. This study assumes that the magnetic field within the blanket region, although varying within about 1T spatially, can be approximated using a characteristic magnetic field. This assumption is important to be able to compare our model results since our MHD methodology only considers the influence of a uniform magnetic field across the system. This methodology is described further in Section 3 as we validate RELAP5-3D using systems with a magnetic field. It is important to note that the characteristic magnetic field within the system is at a strength of 10T at the inboard side. This is much higher than any of the previously investigated systems, however the low flowrate and use of an FCI damp the MHD effects and may be closer to the magnitude of the experimental studies. The temperature values mentioned in this study are design basis values rather than simulated values, but these values should be sufficient for a verification of our model methodology.

The second study by Huang et. al. is a thermomechanical analysis of the channel structural material and gives insight on the temperature gradients of the PbLi and helium within the coolant channels. Some of the parameters of interest within this study are the dimensions of the blanket, flowrates of PbLi and He, and the distribution of temperature within the channels. While we will not be directly using this study for benchmarking our calculated temperature and pressure drop, the insight on the thermal limits is important for the future development of the model. We will need to account for these limits when postulating operation strategies for the system.

LWR AOOs and DBAs for Fusion

The AOOs and DBAs that will be considered for the application to fusion systems will be based on the main categories for LWRs as stated in [34, 63]. The categories are as follows:

- 1) Increase in heat removal by the secondary system
- 2) Decrease in heat removal by the secondary system
- 3) Decrease in reactor coolant system flow rate
- 4) Reactivity and power distribution anomalies
- 5) Increase in reactor coolant inventory
- 6) Decrease in reactor coolant inventory
- 7) Radioactive release from a subsystem or component

The main focus of this analysis will be primarily normal operation as there have been numerous previous analyses concerning accidents within fusion systems, many of which focus on loss of coolant accidents (LOCAs) [13-16, 21-23, 26, 27,

29]. With this in mind, some of the most important transients for the initial operation of a commercial fusion plant would be startup, shutdown, and power ramps. Over the course of these transients, the plant will go through all operational modes of normal operation including power operation, startup, and cooldown [34]. Furthermore, as per NUREG-0800, results of the key parameters for the system must be presented for each of the transients. Specific parameters of interest for this analysis include coolant conditions such as the peak and average core inlet and outlet temperatures, core flowrates, and core pressure differentials. For this study, we will focus specifically on startup transient analysis.

Startup Transients

The startup of a Westinghouse PWR system begins with the system at either cold or hot shutdown conditions as defined by the temperature and pressure of the coolant in the primary loop [64]. Cold shutdown is characterized by depressurization of the reactor coolant system and cooled down coolant temperatures of around 60 °C, which is typically the condition of the reactor following a refueling process. Hot shutdown is characterized by the reactor coolant system staying at temperature and pressure which typically happens following a turbine trip.

The cold shutdown transient begins with the pressurizer being filled and heated to maintain the pressure of the system to prepare to heat the primary loop. The coolant in the primary system is then heated using the heat from the reactor coolant pumps. This allows the reactor to be brought to the hot standby condition where the primary coolant is at the appropriate inlet temperature for operation. This is the starting condition for the hot startup transient. The heating rate of the coolant during this process is limited based on the stress limits on the components of the system from thermal expansion of the coolant which is about 28 °C per hour. The reactor is then brought to criticality using the control rods to a state known as hot zero power (HZP) where the reactor is at temperature and is critical, but the heat is being removed by the turbine bypass system since the turbines have not been loaded. The control rods are then used to drive the power to around 6-15% power at which the turbines are loaded. The power is then driven by the turbine demand and compensated by the control rods to drive the reactor to 100% power at a rate that does not exceed a rate of 5% per minute based on the previously mentioned limitations.

Although standard startup transients of commercial fusion power plants have not been established, several studies have inspected the limitations of startup transients in PbLi tandem mirror systems [65-68]. One key difference to consider between light water cooled and liquid metal cooled systems is the fact that the PbLi coolant in the system is solid at room temperature. This means that in order to initially load the system with PbLi, the pipes will need to be electrically or gas pre-heated to a temperature within about 50 °C of the PbLi inlet temperature to

avoid the coolant from freezing within the pipes and causing initial flow instabilities [66, 68]. Similar to LWRs, the heating rate of the coolant during the startup is limited. This rate is determined by the thermal expansion of the coolant that needs to be accounted for by the surge lines, the stress limits of the materials, and pump limitations due to friction and MHD interactions [65]. Since the FNSF plant design also includes a secondary helium loop and tertiary water loop for steam power generation, pre-heating using pumps or gas will be necessary prior to loading the primary loop to prevent freezing and thermal shock of the structural materials [69].

Several notable experimental startup transients that have been documented for fusion systems include those of the Tore Supra reactor [70-72]. This specific fusion system is significant since during the experimental campaign, the power pulses of the system were very long lasting compared to other experimental facilities such as JET [71]. Plasmas within this system were recorded with times of up to 6 minutes which allows for steady-state plasma analysis [71]. Using the data from the experimental campaign of the Tore Supra system, we can create boundary conditions for the relative power of the plasma during such a startup. It is important to understand that the experimental data from this particular system will be used solely to verify that the RELAP5-3D model of the DCLL system is capable of obtaining transient results and to record outlet temperatures for the system. The Tore supra system is a pulsed fusion system that is not built for the generation of electricity, but for studying the phenomena of the plasma and plasma facing components specifically for long term plasma operation [72]. This means that the system can operate without the thermal stress limitations of the tandem mirror systems which account for the heat transfer from the plasma to a liquid.

As seen in the experimental campaign, the typical shape for this type of power pulse is a nearly instantaneous transition from 0% power to 100% power with a long lasting steady-state operation period and subsequent instantaneous drop in power from 100% to 0% [72]. In both the startup and shutdown of the system, the rate of change of the power vastly exceeds the previously established limits for systems such as the Westinghouse PWR at about 5% per minute [64]. The relative power transient that we will be using for the startup transient for the DCLL system is a simulated startup transient of Tore Supra using ITER power conditions with the same pulse shape as the Tore Supra system [70]. This will be converted to a normalized power curve and heat will be applied to the blanket system using a heating profile that is scaled to the power of the FNSF design. The relative power transient for Tore Supra is shown in Figure 2.7, and a more realistic startup transient using the maximum rate of 5% power per minute is shown in Figure 2.8. We can see that the time it would take for a startup procedure following the thermal stress limitations takes 20 minutes at a maximum heatup rate which would likely be longer in reality due to large thermal

gradients, and startup occurring in sequences for turbine loading such as within a PWR system. Realistically, startup would probably occur over a day with several procedural tests and power stages such as within the tandem mirror systems [67].

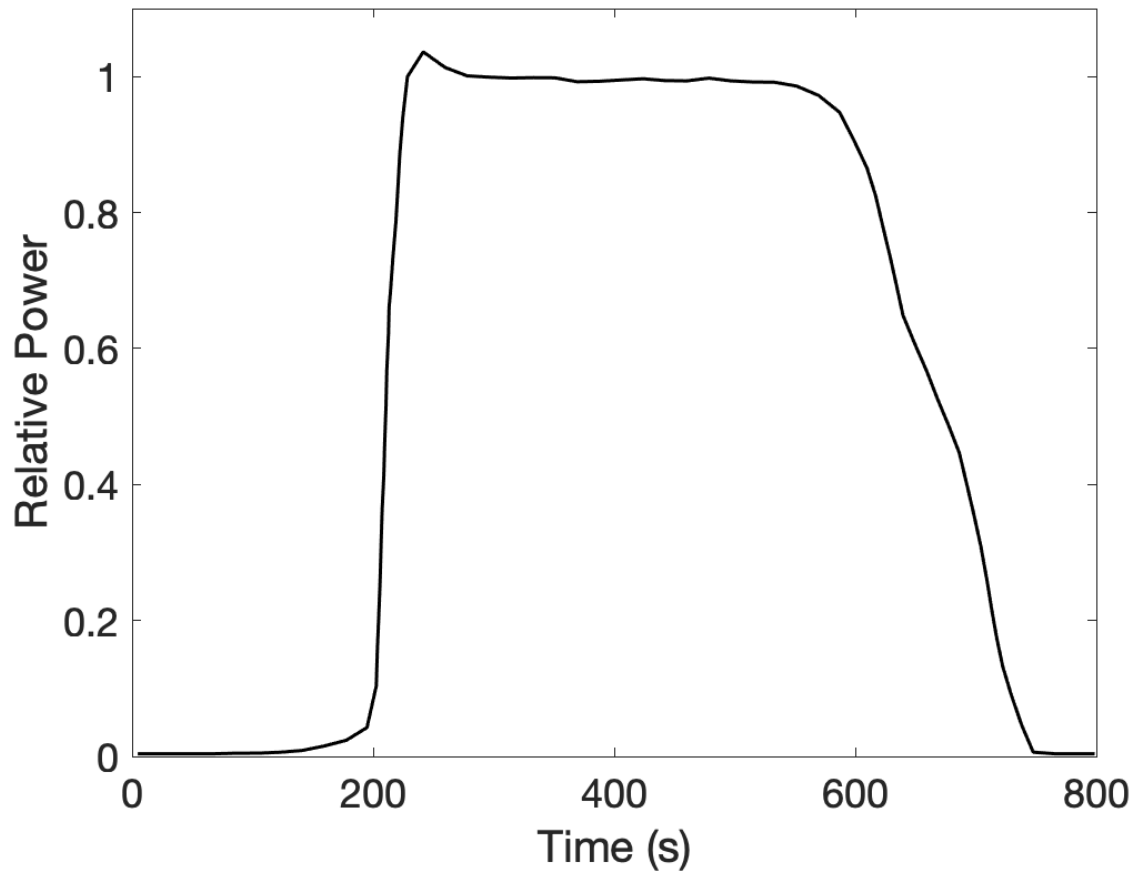


Figure 2.7. Normalized Tore Supra Power Pulse Based on Experimental Campaign [70]

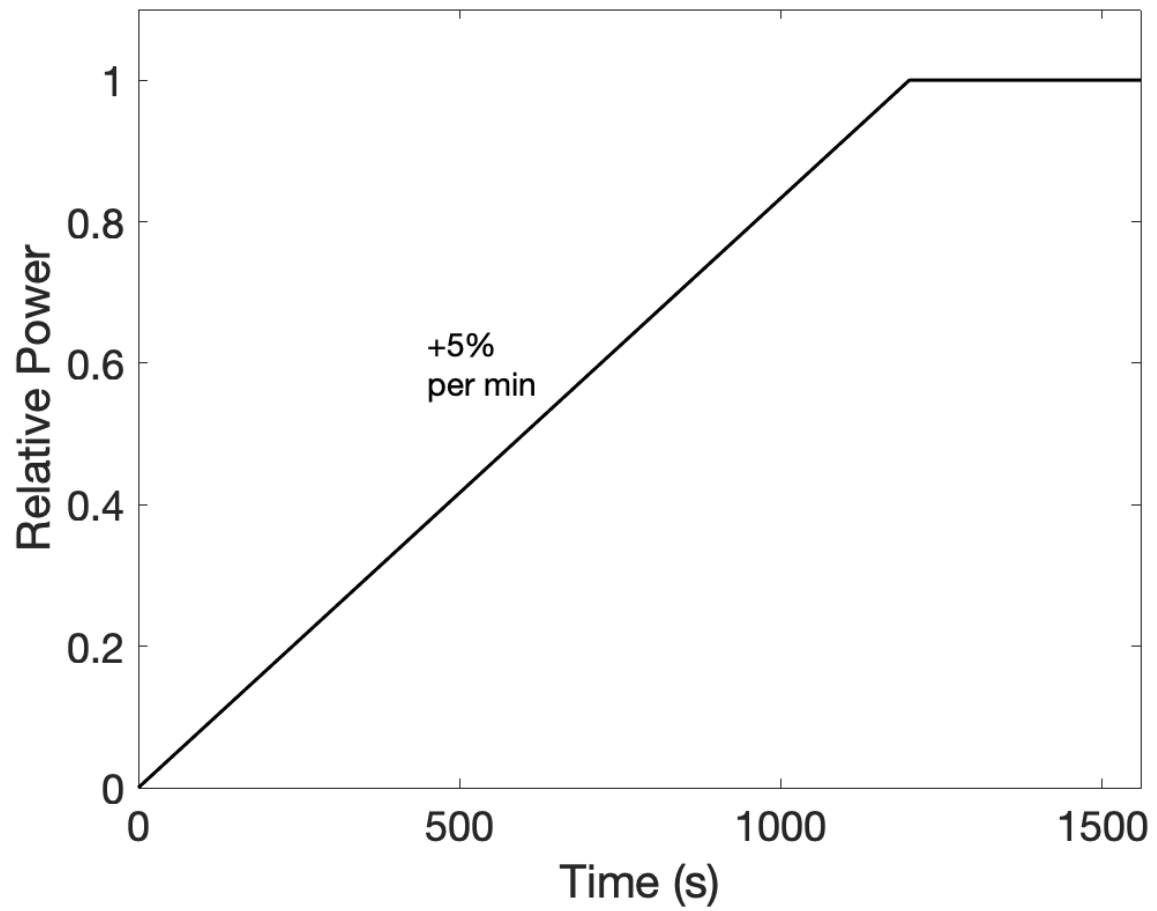


Figure 2.8. Representative Normalized Startup Transient Based on Thermal Stress Limitations

CHAPTER THREE

VALIDATION BASIS FOR RELAP5-3D

Representative Flow Loop

Background and Methods

The first step we took in demonstrating the modeling capabilities of RELAP5-3D was the construction of a vertical flow loop model using PbLi as the working fluid. A nodalization diagram, pipe lengths and selected operational conditions of the loop model are shown in Figure 3.1. This model consisted of a closed loop of square channel pipes with single volumes acting as corners. The flow within the system is controlled using a time-dependent junction which is a component that connects two volumes and maintains a constant flowrate between them. The time-dependent junction for this system connects volume 203, the volume just before the heated vertical pipe, and 100-1, the first volume of the heated vertical pipe. All other pipes and volumes within the model are connected by single junctions with flowrates that are calculated during the simulation. A heat structure is attached to the vertical pipe following the time-dependent junction, which is kept at 1000 K and acts as the heat source for the system. A corresponding heat sink is attached to pipe 102 on the other side of the loop in the form of a heat structure that is kept at a constant temperature of 200 K. In order to keep the pressure stable as the system approaches a steady state, a pressurizer (volume 400 in Figure 3.1) in the form of a time-dependent volume is attached to the system. A time dependent volume is a volume that stays at a constant temperature and pressure and in this case is kept at atmospheric pressure and the initial loop temperature of 600K. All components within the loop are insulated from the outside environment and heat transfer only occurs between the heat source and heat sink. Flow areas between each volume are also kept constant so there are no pressure drops due to forms losses between pipes and junctions. Flow within this model is assumed to be fully developed.

Results

Null transients were performed to inspect the pressure and temperature within the system. Since a previous study has determined that the thermophysical properties within RELAP5-3D are not accurate to experimental data due to the equation of state within the property files [73], heat transfer and pressure drop calculations were performed using both the properties from RELAP and a literature review by Martelli et. al. [74]. An example transient response can be seen in Figure 3.2, which shows the approach to steady state of the temperature change across the hot leg. This transient is compared to an analytical average heat transfer calculation using the relation $Q = \dot{m}C_p\Delta T$ calculated using both properties.

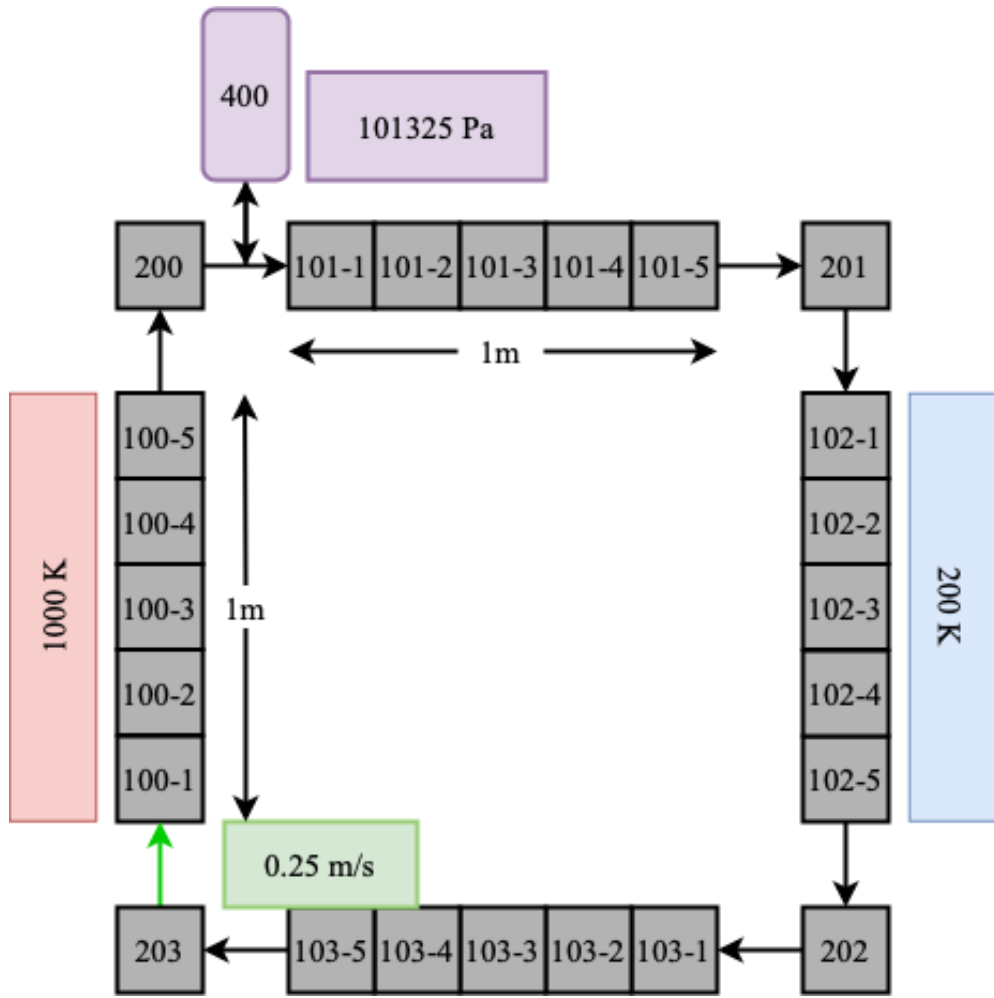


Figure 3.1. Representative Flow Loop Nodalization

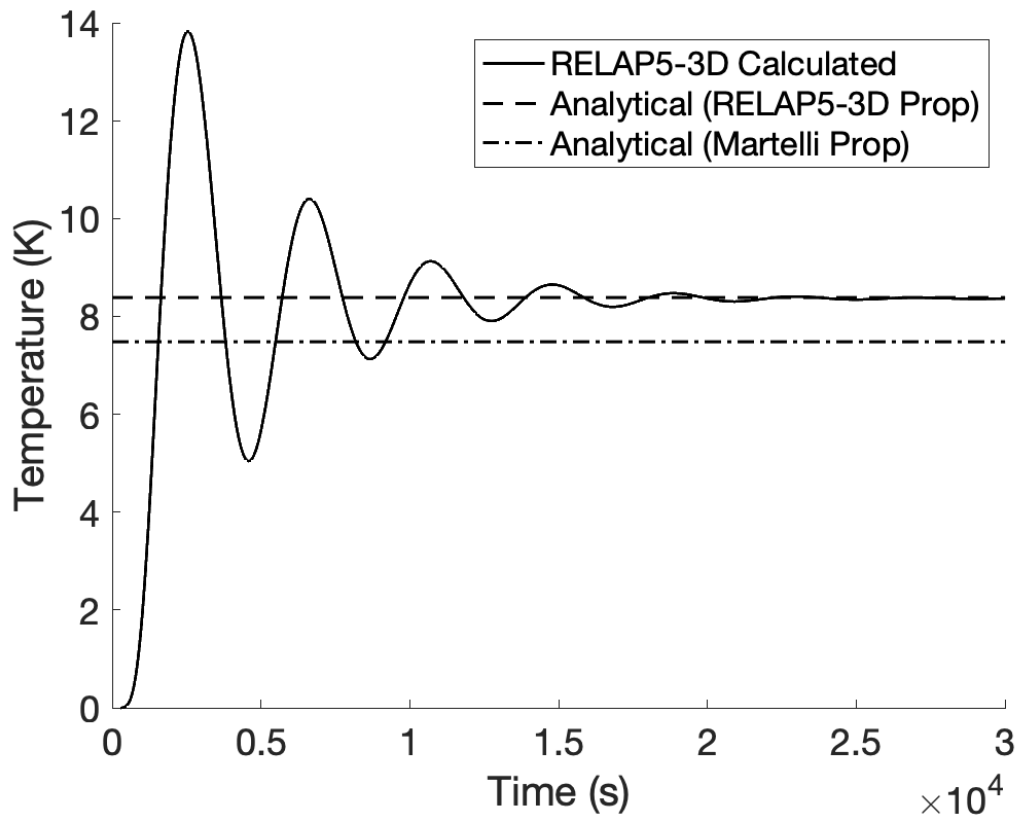


Figure 3.2. Representative Flow Loop Transient Temperature Difference Across Hot Leg

The average heat flux for the analysis is taken from the null transient heat flux across the hot leg shown in Figure 3.3 and is the average between the heat flux in the first and last volumes as calculated by RELAP5-3D. Table 3.1 contains the data used in the analytical calculation.

From this analysis, we are able to determine that the calculation in RELAP5-3D converges to the analytical value of 8.38 K while the calculation using the literature review values is 7.48 K which gives a relative error of 12.1%. We also calculated the gravitational pressure drop, $\Delta P = \rho gh$, associated with the change in height of 1m to be around 0.08879 MPa using the RELAP5-3D properties which has good agreement with the model calculation of 0.08877 MPa, but has a relative error of 7.7% compared to the literature review calculation of 0.096 MPa. With this, we determine that RELAP5-3D is sufficient in capturing the heat transfer and pressure phenomena of PbLi systems without the influence of a magnetic field, but there will be potential discrepancies between the RELAP5-3D calculations and the experimental values.

Natural Circulation Loop (ORNL)

Background and Methods

Several natural circulation corrosion loops using PbLi have been constructed at ORNL inspecting the compatibility of an Iron-Chromium-Aluminum (FeCrAl) alloy for use as fusion system structural material [75-77]. A diagram of the loop design can be found in Figure 3.4. Experiments within these loops inspect corrosion of chains of tensile specimens following 1000h of steady state flow conditions and are conducted at temperatures ranging from 773.15-923.15 K. A recent paper [75] focused on development and validation of a high fidelity model within COMSOL for analysis of temperature fields and fluid flow of these PbLi corrosion loops using experiment-relevant temperature conditions. We developed a RELAP5-3D ROM for the PbLi loop based on the data from the preliminary experimental campaign of the corrosion loop and the developed high fidelity model [75, 76]. This model will be validated using the experimental flow conditions. Specific measurements for the loop can be found within Table 3.2. and a nodalization diagram of the RELAP5-3D model can be seen in Figure 3.5.

The flow of PbLi within the model is driven by natural circulation. The buoyancy force from the positive temperature gradient across the hot leg drives the flow up the vertical section and the heat is then lost through conduction and radiation as it passes through the cold leg. Once the system reaches steady state, the heat applied to the hot leg is equivalent to the heat lost in the cold leg. To emulate the heat sources and sinks within these models, heat structures were applied to each pipe within the loop. The hot leg heat structure consists of a convective boundary on the channel side and an insulated boundary for the surroundings.

Table 3.1. Representative Flow Loop Operational Conditions

| Parameter | | Value | Units |
|---------------------------|--------|--------------------|--------------|
| Initial Temperature | T | 600 | K |
| Average Hot Leg Heat Flux | q'' | 1.23×10^4 | W/m^2 |
| Fluid Velocity | v | 0.001 | m/s |
| Channel Flow Area | A | 0.5 | m |
| Channel Length | L | 0.8 | m |
| Fluid Density (RELAP) | ρ | 9051.74 | kg/m^3 |
| Fluid Density (Martelli) | ρ | 9805.96 | kg/m^3 |
| Specific Heat (RELAP) | C_p | 183.18 | $1/\Omega m$ |
| Specific Heat (Martelli) | C_p | 189.53 | $1/\Omega m$ |

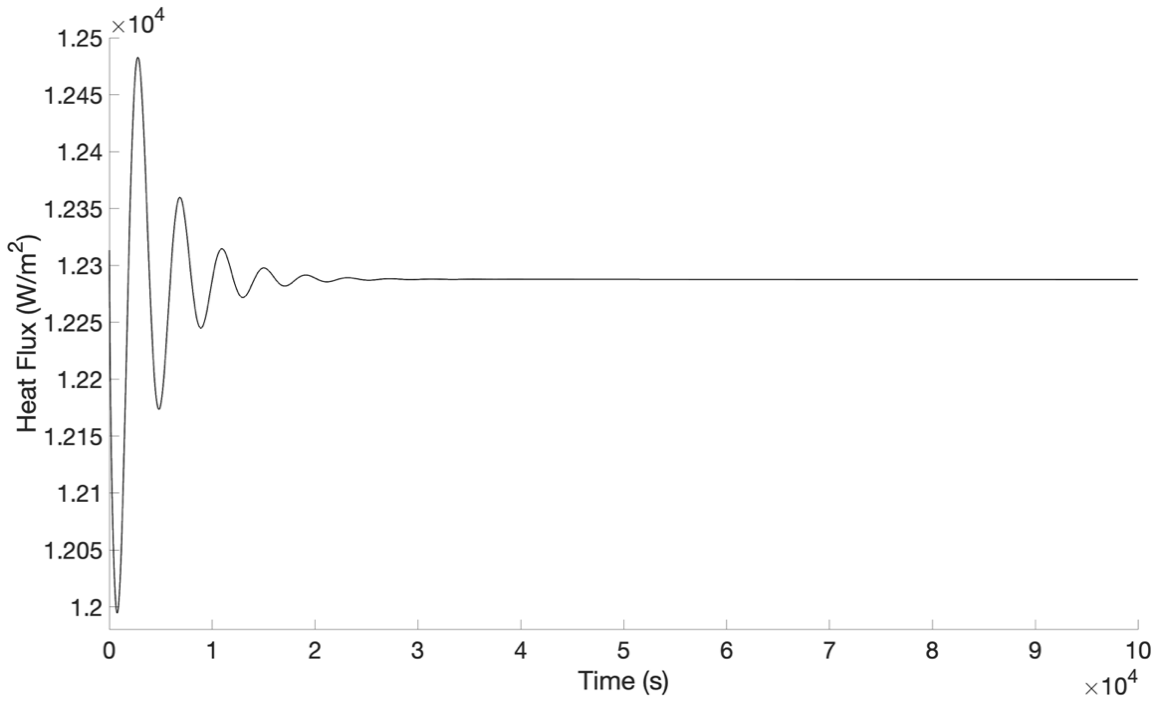


Figure 3.3. Representative Flow Loop Transient Average Heat Flux Across Hot Leg

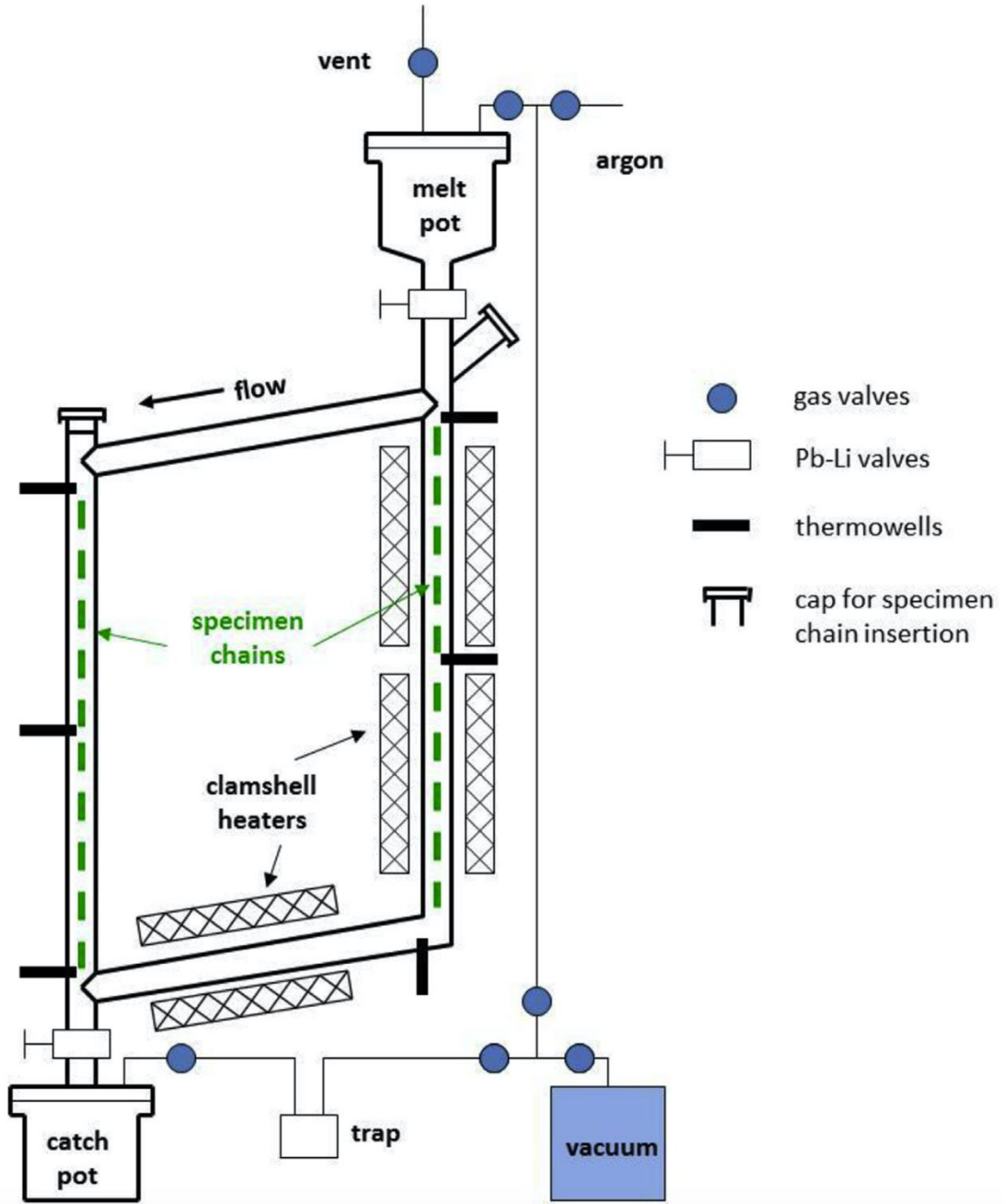


Figure 3.4. Natural Circulation Loop Design

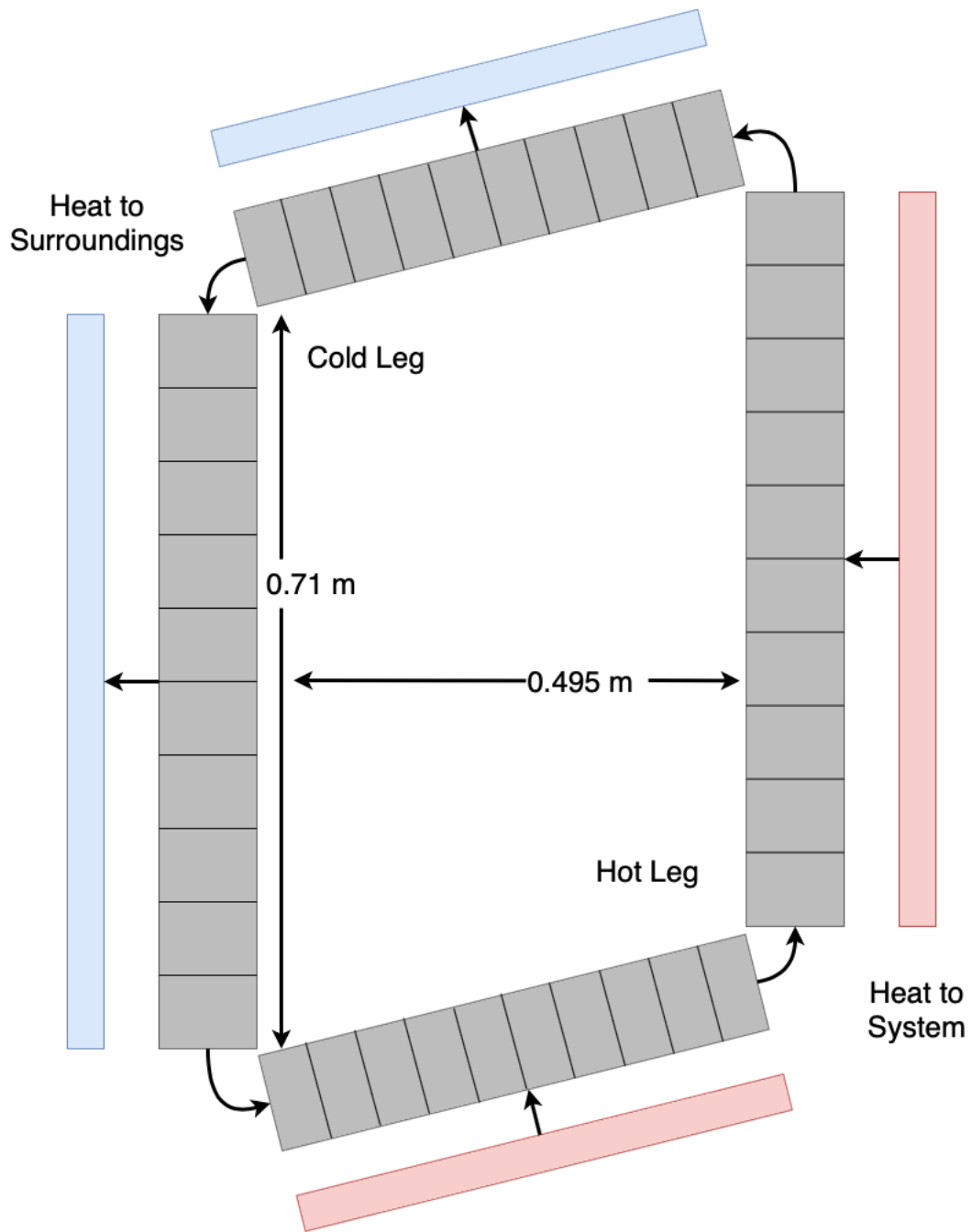


Figure 3.5. Natural Circulation Loop Nodalization Diagram

Table 3.2. Natural Circulation Loop Model Specifications

| Parameter | Value | Units |
|--|--------------|---------------------|
| Horizontal Spacing | 0.495 | m |
| Vertical Spacing | 0.71 | m |
| Horizontal Slope | 1:4 | N/a |
| Pipe Outer Diameter | 0.0267 | m |
| Pipe Wall Thickness | 0.0031 | m |
| Loop Average Temperature | 745 | K |
| PbLi Density (ρ) | 8922.9 | Kg/m ³ |
| PbLi Specific Heat (c_p) | 178 | J/Kg*K |
| Horizontal Hot Leg Power (Q) | 129.9 | W |
| Vertical Hot Leg Power (Q) | 558.9 | W |
| Curve Fit Parameter 1 (a) | -.006372 | N/a |
| Curve Fit Parameter 2 (b) | .5521 | N/a |
| Curve Fit Parameter 3 (c) | .06654 | N/a |
| Forms Loss Coefficient (K) | 58 | N/a |
| Effective Heat Transfer Coefficient (h) | 12 | W/m ² *K |

The cold leg heat structure consists of a convective boundary on both the channel side and on the surrounding side. These heat flux applied across the hot leg was calculated using the relationship $Q = \dot{m}C_p\Delta T$ using thermal properties of PbLi taken from the RELAP5-3D code and at the nominal flow rate within the loop to achieve the desired temperature change across the hot leg. As stated in [75], the pressure drop coefficient due to the inclusion of the tensile chains can vary greatly during experimental testing, suggesting that the additional friction caused is not negligible. To account for this additional forms loss, I applied a curve fitting to the forms loss coefficient parametric study performed on the high fidelity model [75]. The curve fit of the form $a+bx^c$ can be shown in Figure 3.6. and shows the model flowrate corresponding to different forms loss pressure drop coefficients. This data was extrapolated to the experimental flow rate of 0.0067 m/s and a forms loss coefficient of 58 was determined. The heat transfer from the cold leg to the surroundings consists of both convective and radiative heat transfer; as determined by [75]. This is implemented into the heat structure using an equivalent heat transfer coefficient. This coefficient was determined iteratively and found to have a value of 12 W/m²K.

Results

The temperature and flow velocity of the model during a null-transient simulation are shown in Figures 3.7 and 3.8, respectively. Table 3 contains a comparison of the model and experimental flow parameters. The heat transfer coefficient of 12 W/m²K is noticeably lower than that of the COMSOL model's value of 45 W/m²K, but this is to be expected since the flow velocity and the heat applied across the hot leg are both an order of magnitude higher than the model. The model velocity under natural circulation conditions with the forms loss applied is 0.0065 m/s which has a relative error of 3% with the experimental value of 0.0067 m/s as reported in [76]. The steady state loop temperatures within the model converge to within 5 K of the experimentally measured temperatures as reported in Table 3. From the results of this study, I validated the RELAP5-3D model and determine that RELAP5-3D ROMs produce accurate results for heat transfer and pressure effects within PbLi systems without the influence of a magnetic field.

ALEX Facility (ANL)

Background and Methods

The ALEX facility was constructed to perform 3-D MHD analysis in support of tokamak blanket research [43]. The working fluid for the ALEX facility at the time of these experimental results was liquid NaK, which behaves similarly to PbLi under MHD conditions [55]. The goal of the loop was to obtain experimental analysis of 3-D flow profiles under MHD conditions since at the time there was very limited experimental data to use for developing analysis codes [43].

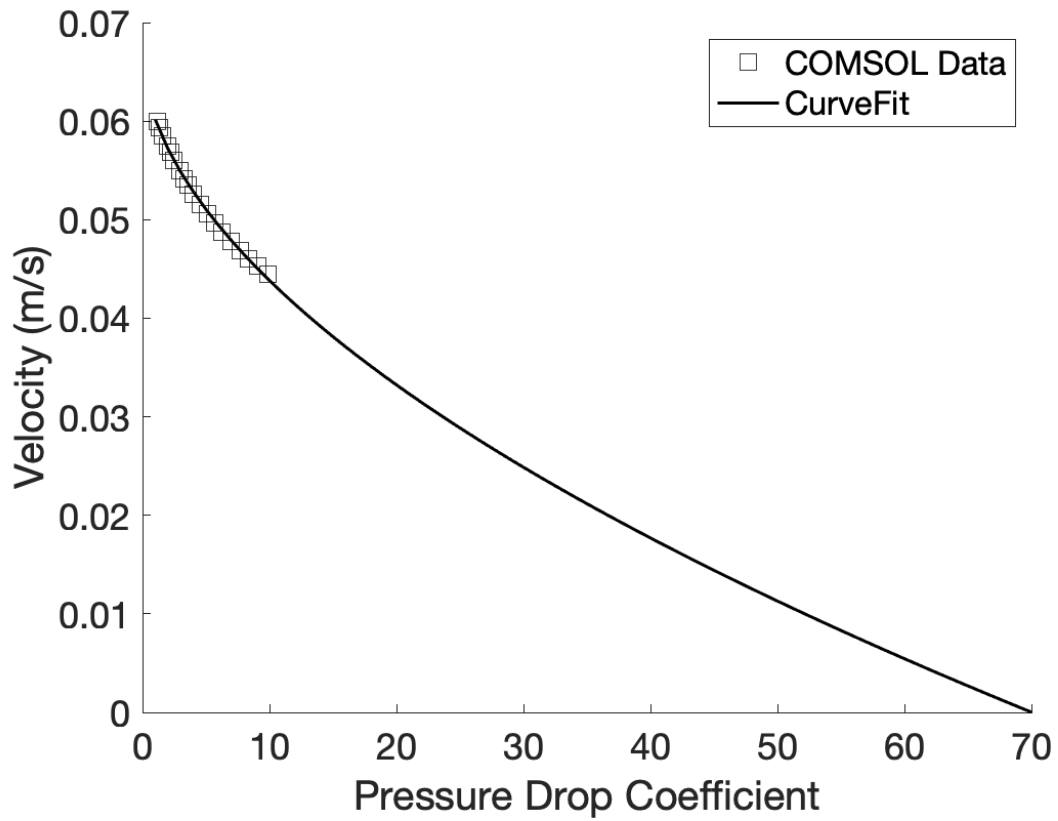


Figure 3.6. Forms Loss Coefficient Curve Fit Using Parametric Data [75]

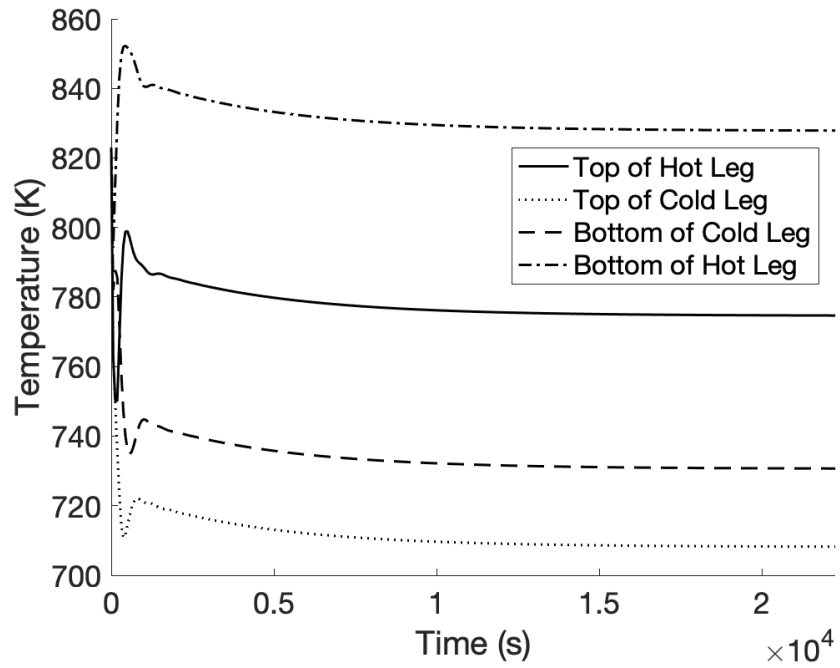


Figure 3.7. Natural Circulation Loop Null Transient Temperature Distribution

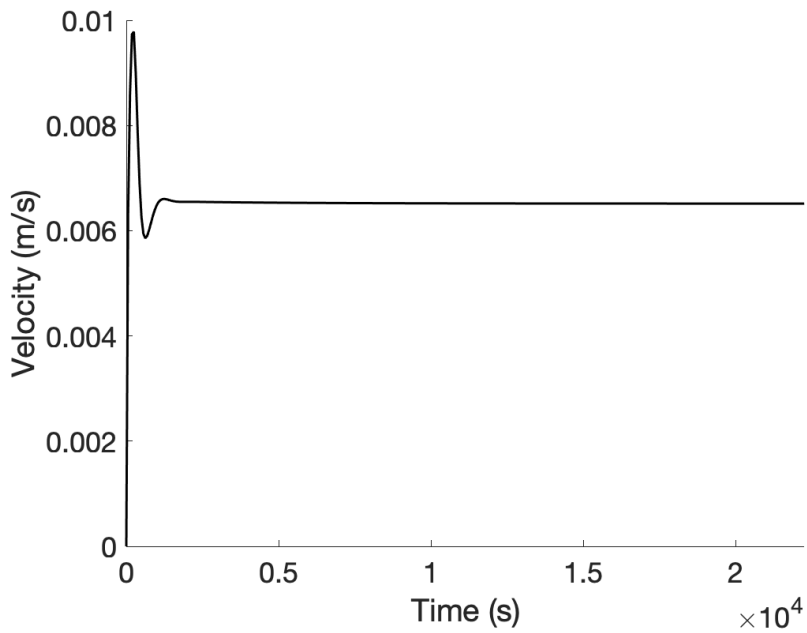


Figure 3.8. Natural Circulation Loop Null Transient Flow Velocity

Table 3.3. Natural Circulation Loop Steady State Flow Parameters

| Parameter | Model | Experimental | Units |
|---------------------------------------|--------------|---------------------|--------------|
| Top of Cold Leg Temperature | 774.6 | 769.6 | K |
| Bottom of Cold Leg Temperature | 708.1 | 707.5 | K |
| Bottom of Hot Leg Temperature | 730.6 | 729.3 | K |
| Top of Hot Leg Temperature | 827.7 | 823.2 | K |
| Flow Velocity | .0065 | .0067 | m/s |

ALEX has since been benchmarked as one of several facilities for validating high fidelity 3-D MHD codes for fully developed flow for a uniform and fringing transverse magnetic field under square and circular pipe geometries as detailed in [48] and explained further in Section 2. A detailed description of the ALEX facility at the time of the benchmarking experiments can be found in [43] and a layout of the experimental flow loop can be seen in Figure 3.9. The simplified model of the ALEX facility built in RELAP5-3D is shown in Figure. 3.10, which solely includes the MHD test section of the loop.

Experimental data from the ALEX facility was previously used for the validation of MHD pressure drop within the ATHENA code with two different methodologies [54, 55] for use in ROMs. The ATHENA code is a transient thermal-hydraulic code that was developed specifically for fusion system analysis. The first method for MHD analysis used a relation to directly calculate the pressure drop over the length of a uniform or fringing field [54]. The second method implemented the use of an equivalent wall friction factor that could be used within the continuity equations [55]. Our implementation of MHD pressure drop will follow the methodology of the second ATHENA code validation since we can add the effect as an external friction factor which requires no change to the RELAP5-3D source code.

The RELAP5-3D code allows users to specify a frictional loss coefficient for various flow phenomena. The MHD pressure drop was implemented as a user-input loss coefficient given by Eq. (1) and is based on the formulation in [55]. Operational parameters for the ALEX experiments which are necessary to calculate the MHD pressure drop are included in Table 3.4. The Hartmann number, M , is defined as a ratio of the electromagnetic force to the viscous force within the flow in Eq. (2). ϕ is the ratio of the wall electrical conductivity times the wall thickness to the fluid electrical conductivity times the channel half-width contained in Eq. (3). The parameter δ is dependent on whether the channel geometry is circular or square and is either 0 or a value based on interpolation of tables as described in [55], respectively. The parameter f_{config} is dependent on whether the volume is within a uniform or fringing magnetic field and is either 1 or calculated using the relation in [55], respectively. The equivalent friction factor uses the friction factor relationship within the RELAP5-3D phasic momentum equations. A conversion factor based on the velocity, v , and pipe volume length, Δx , allows the MHD pressure effect to be implemented as a frictional loss. The channel geometry within the RELAP5-3D model was set to be circular, and a uniform magnetic field was used throughout the entire test section.

$$FWF_{\text{MHD}_{\text{NEW}}} = \left[\frac{2\Delta x}{v} \right] \left[\frac{1}{\rho_f} \right] \left[\frac{1}{M-1} + \frac{\phi}{1+\phi+\delta} \right] f_{\text{config}} \sigma_f B^2 \quad (1)$$

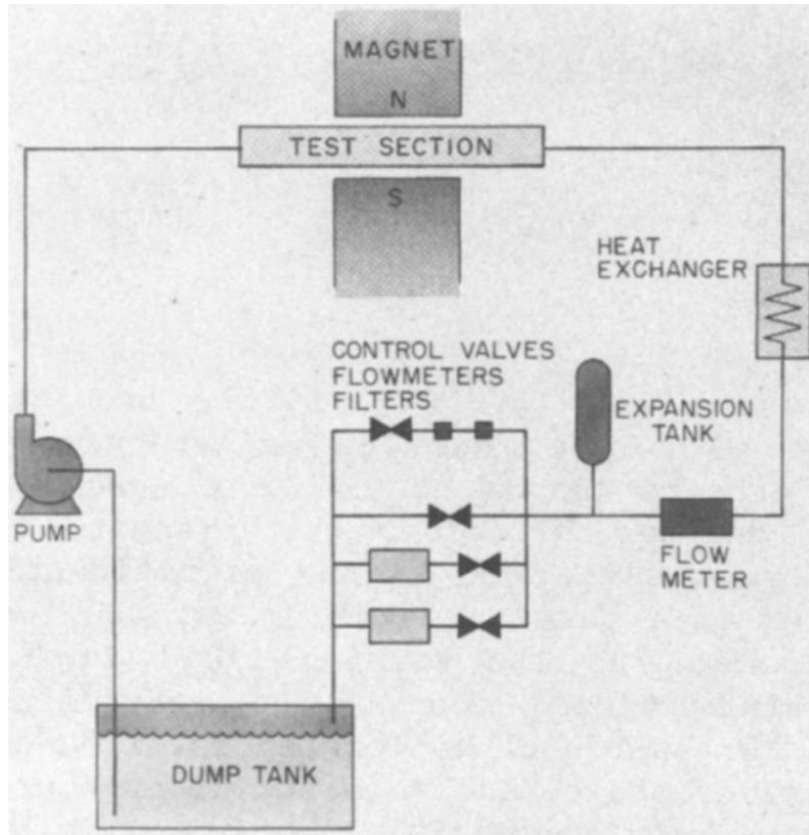


Figure 3.9. ALEX Facility Loop Design

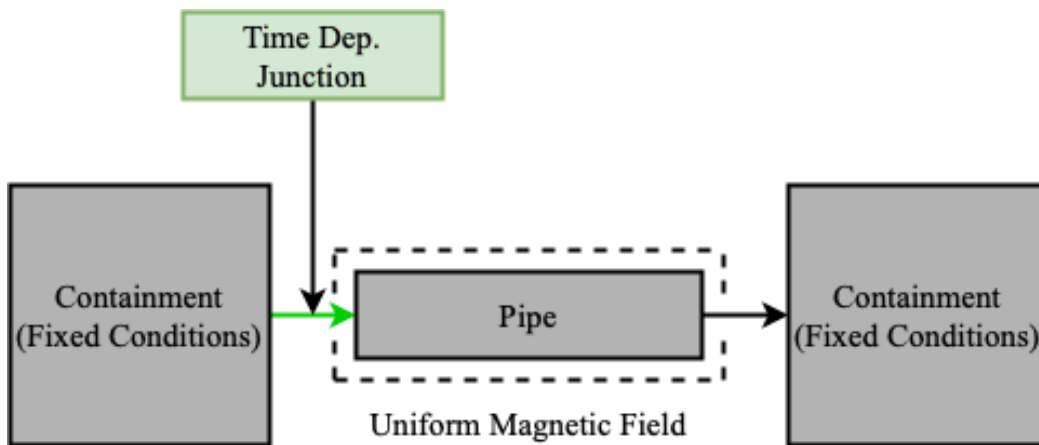


Figure 3.10. ALEX Facility Nodalization Diagram

Table 3.4. ALEX Facility MHD Parameters

| Parameter | | Value | Units |
|-------------------------------|---------------------|-----------------------|-------------------|
| Field Strength | B | 2 | T |
| Fluid Velocity | v | 0.07 | m/s |
| Channel Half-Width | a | 0.044 | m |
| Wall Thickness | t_w | 0.0066 | m |
| Fluid Electrical Conductivity | σ_f | 2.83×10^6 | 1/ Ω m |
| Wall Electrical Conductivity | σ_w | 1.31×10^6 | 1/ Ω m |
| Fluid Density | ρ_f | 839 | kg/m ³ |
| Fluid Dynamic Viscosity | μ_f | 1.80×10^{-3} | Pa*s |
| Volume Length | Δx | 0.541 | m |
| Channel Geometry Parameter | f_{config} | 1 | n/a |

$$M = BL \sqrt{\frac{\sigma_f}{\mu}} \quad (2)$$

$$\phi = \frac{\sigma_w t_w}{\sigma_f a} \quad (3)$$

Results

We compared our implementation of the MHD pressure drop effect in RELAP5-3D to data within the ATHENA validation study and the international benchmark study. The pressure relative to the inlet pressure across the length of the MHD test section for the ATHENA benchmark case is shown in Figure 3.11. The calculated pressure distribution from the RELAP5-3D simulation showed excellent agreement with the verification data from the ATHENA calculation. The small discrepancies in pressure drop across the first and last volumes are from the transition from a uniform magnetic field to a fringing magnetic field, which we did not consider in our model. As expected, the pressure drop within these fringe field regions was larger for the RELAP5-3D calculations since the strength of the uniform magnetic field is stronger than the fringing field volumes in the experimental data.

By expressing the results from this validation study using the dimensionless parameters from Section 2, we can compare our results to the international benchmark study. We see that the data closely matches those of high fidelity 3-D codes within the uniform magnetic field region with a relative error of 4.5% to the experimental results. The calculated Hartmann number and interaction parameter for this test are 6831 and 10428 which has a relative error of 3.5% and 2.5% with the benchmark values of 6600 and 10700, respectively. The comparison to the benchmark MHD pressure drop data is shown in Figure 3.12. From this data, we observe that our implementation of MHD pressure drop phenomena is accurate under uniform field conditions at this field strength and flow rate, but it needs further validation across a wider range of system conditions.

MaPLE Loop (UCLA)

Background and Methods

The MaPLE facility was constructed at UCLA for the experimental analysis of 3-D MHD effects and FCI performance [78]. Experimental MHD tests have previously been performed investigating pressure drop under a uniform magnetic field, fringing magnetic field, and under several FCI design variations [78]. MHD effects have been investigated under steady state conditions using a variety of experimental setups using high fidelity numerical 3-D CFD analysis. Of the experimental campaigns, we chose to use data from the initial MHD pressure drop experiments without the use of an FCI.

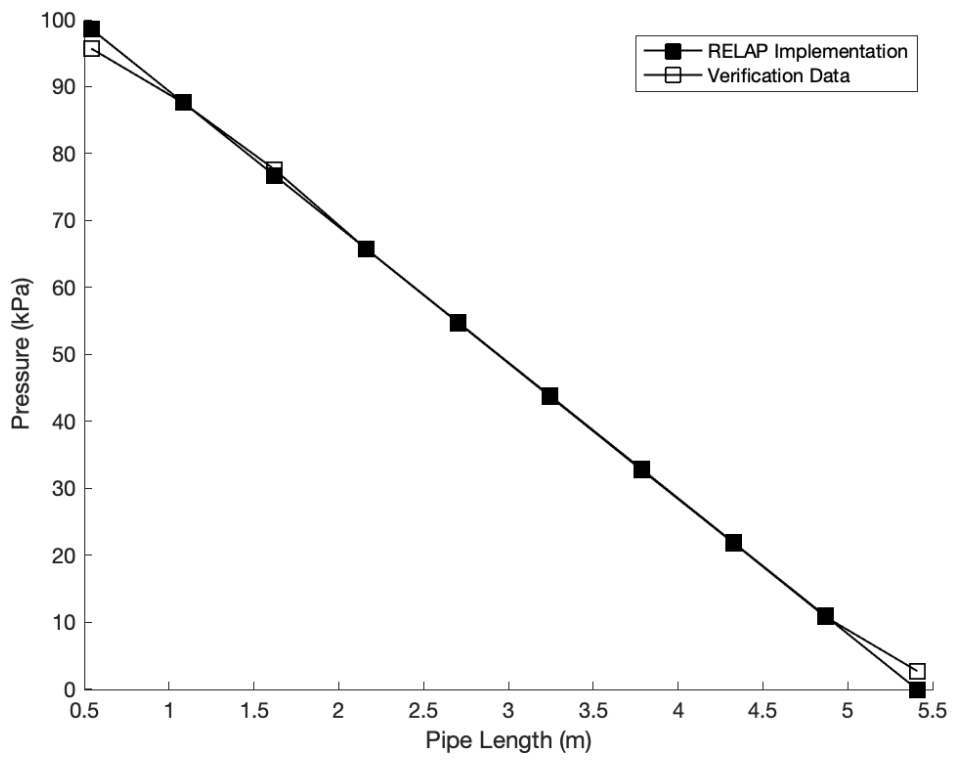


Figure 3.11. ALEX Facility Pressure Distribution Relative to Inlet Pressure

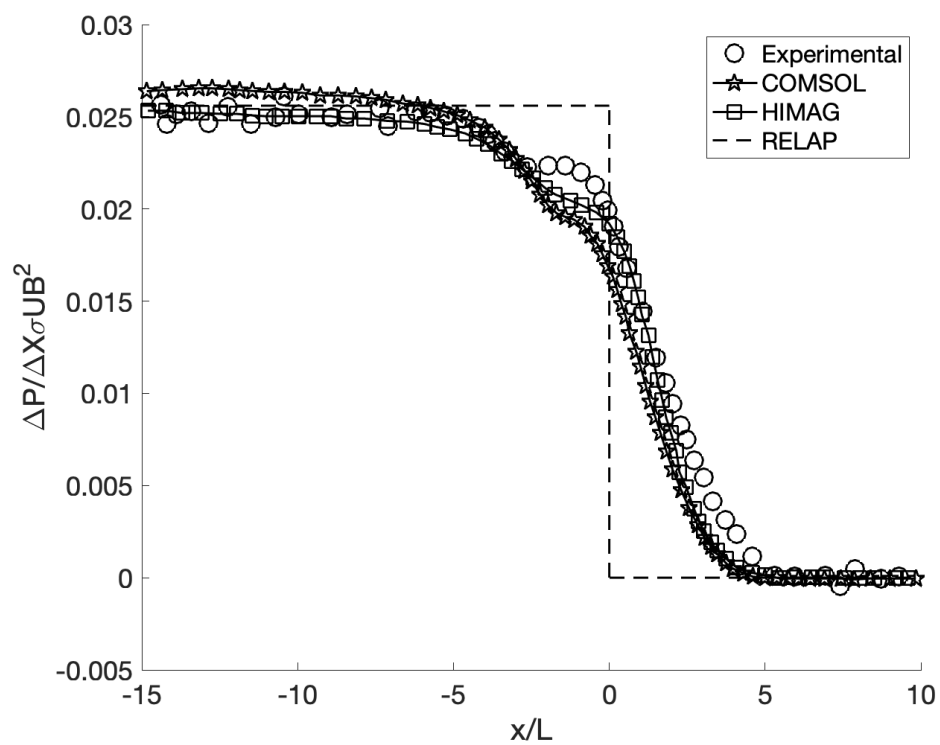


Figure 3.12. ALEX Facility Dimensionless Pressure Drop for Circular Channel Geometry

The experiment was run using a bare round channel with fully developed flow under a uniform magnetic field. This satisfied the conditions for using our MHD implementation using the expression formulated in the ALEX validation study and will allow us to verify the implementation under several velocities and magnetic field strengths. A diagram of the MaPLE loop design is shown in Figure 3.13.

A simplified model of the MaPLE loop was constructed in RELAP5-3D to perform an experimental comparison study. The model used specific test section data from [44] and rough estimations for the remaining components based on corresponding reference images. These approximations are deemed reasonable since the main focus is on the MHD pressure drop across the test section. The flow within the model was kept constant using a time-dependent junction representing the electromagnetic pump, and the pressure was stabilized using a pressurizer similar to the component implemented in the representative flow loop model, which acted as the vacuum pump. The magnetic field across the test section in each case was uniform and applied in the transverse direction. A detailed description of the MaPLE loop and its components can be found in [44] and the nodalization diagram of our RELAP5-3D model is shown in Figure 3.14. The RELAP5-3D calculations will be compared to both the experimental data and an analytical correlation for pressure drop within a circular channel with thin conducting walls developed by Miyazaki et. al. [61]. The MHD correlation by Miyazaki is given by Eq. 4, where ϕ is the ratio of the wall electrical conductivity times the total wall thickness to the fluid electrical conductivity times the channel half-width as defined by Eq. 3.

$$\Delta P = L \left[\frac{\phi}{1 + \phi} \right] \sigma_f v B^2 \quad (4)$$

Specifications of the test section and the fluid properties of PbLi used in the model calculations and analytical correlation can be found in Table 3.5.

Results

Figure 3.15 contains the full comparison between all the magnetic field strength cases using the MHD coefficient calculated with the RELAP5-3D property file. Figure 3.16 contains another full comparison between all the magnetic field strength cases using the MHD coefficient calculated with the literature review PbLi property data. Table 3.6 contains the change in pressure drop over the change in velocity for each of the calculated correlations. Table 3.7 contains the relative error in the magnitude of the MHD pressure drop calculations to the experimental data. Table 3.8 contains the error in the change in pressure over change in velocity of the RELAP5-3D calculations to the other models. The magnitude of the MHD pressure drop calculated using the literature review properties of PbLi tend to agree better than the RELAP5-3D properties at lower magnetic field strengths.

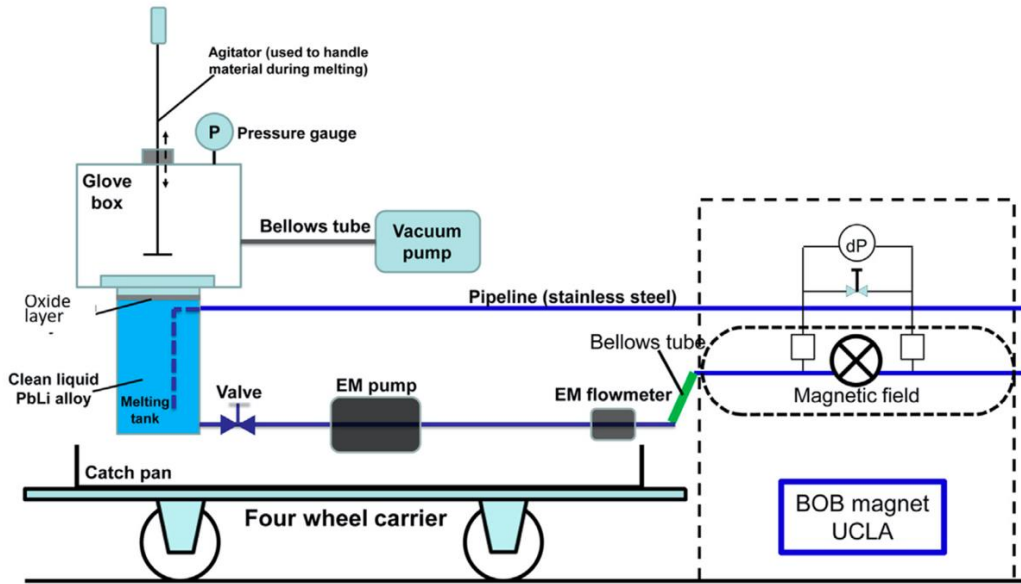


Figure 3.13. MaPLE Loop Design

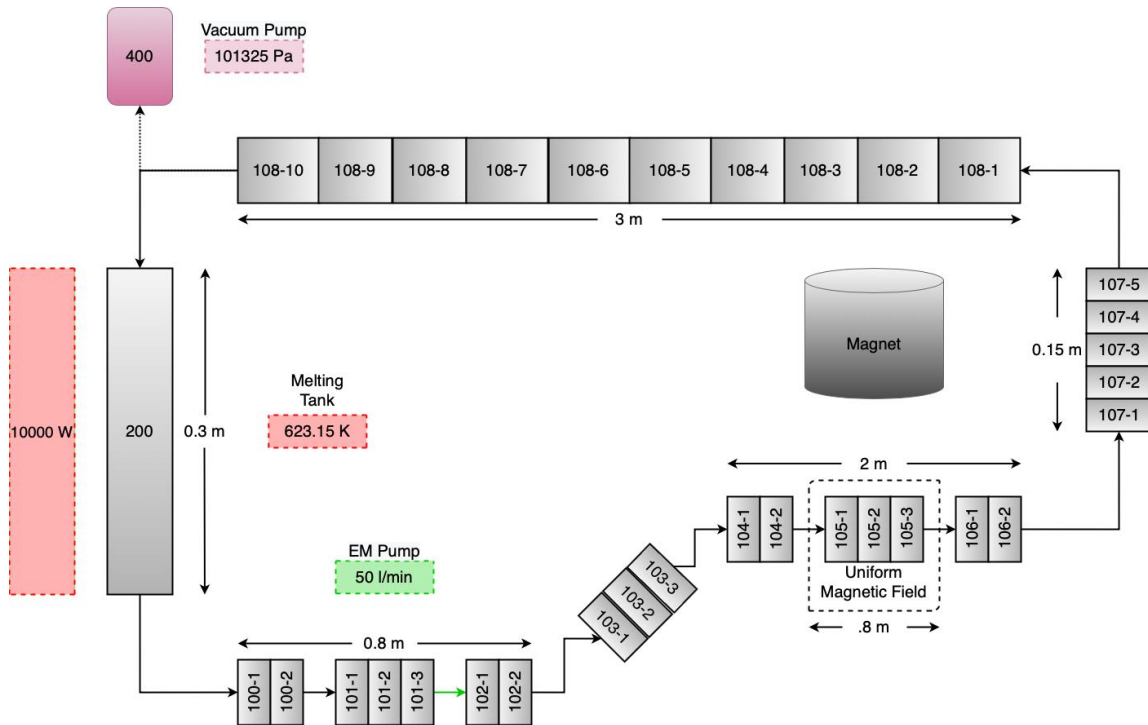


Figure 3.14. MaPLE Loop Nodalization Diagram

Table 3.5. MaPLE Loop MHD Parameters

| Parameter | | Value | Units |
|--|---------------------|------------------------|-------------------|
| Temperature | T | 623.15 | K |
| Channel Half-Width | a | 0.0111 | m |
| Wall Thickness | t_w | 0.0024 | m |
| Fluid Electrical Conductivity [74] | σ_f | 8.67×10^5 | 1/ Ω m |
| Wall Electrical Conductivity 1 [79] | σ_w | 1.052104×10^6 | 1/ Ω m |
| Wall Electrical Conductivity 2 [80-83] | σ_w | 1.050751×10^6 | 1/ Ω m |
| Fluid Density (RELAP5-3D) | ρ_f | 9032 | kg/m ³ |
| Fluid Density [74] | ρ_f | 9778 | kg/m ³ |
| Fluid Dynamic Viscosity (RELAP5-3D) | μ_f | 1.80×10^{-3} | Pa*s |
| Fluid Dynamic Viscosity [74] | μ_f | 1.13×10^{-3} | Pa*s |
| Volume Length | Δx | 0.05 | m |
| Total Channel Length | L | 0.5 | m |
| Channel Geometry Parameter | f_{config} | 1 | n/a |

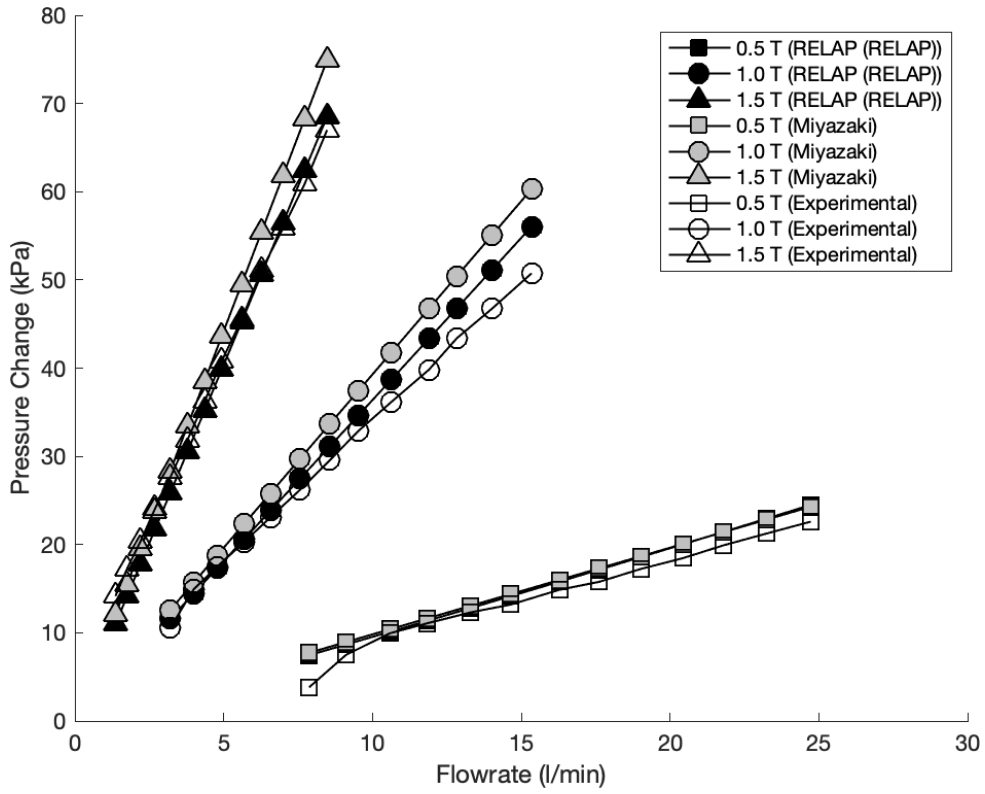


Figure 3.15. MHD Pressure Drop Across Uniform Field Test Section using RELAP5-3D Properties

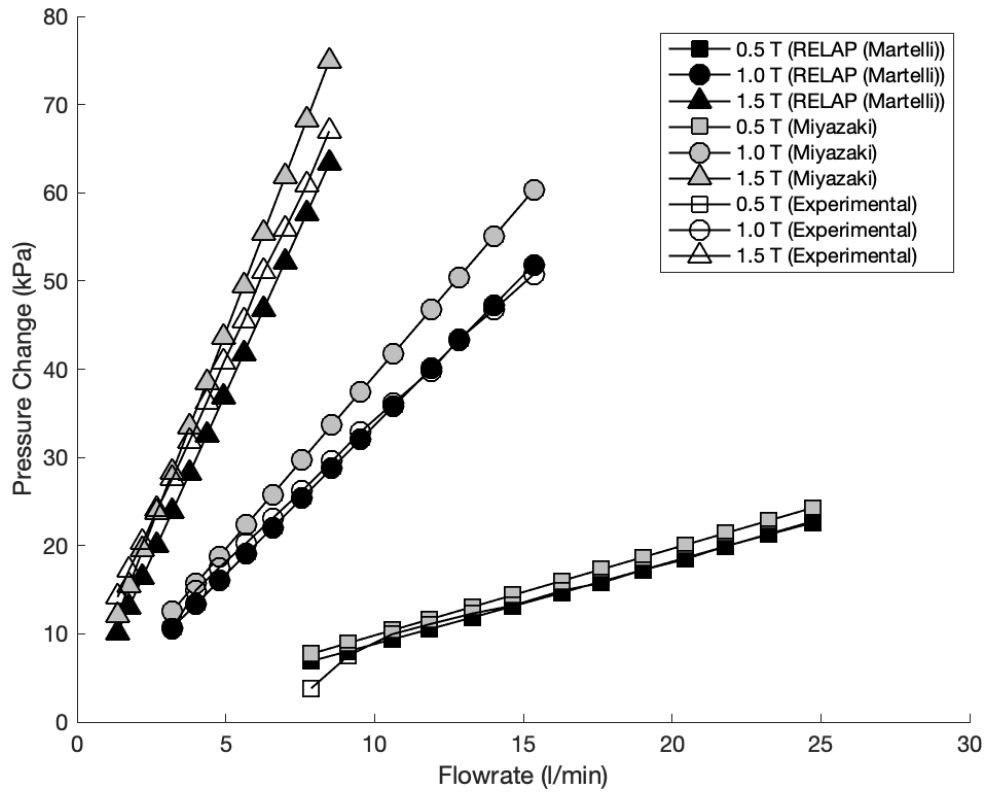


Figure 3.16. MHD Pressure Drop Across Uniform Field Test Section Using Literature Review Properties from [74]

Table 3.6. MaPLE Loop Change in MHD Pressure Vs Change in Flow Rate

| Case | dP/dv (Experimental) | dP/dv (RELAP5-3D) (RELAP5-3D Properties) | dP/dv (RELAP5-3D) (Literature Review Properties) | dP/dv (Miyazaki) |
|--------------|---------------------------------|--|--|-----------------------------|
| 0.5 T | 1.00 | 1.01 | 0.94 | 0.98 |
| 1.0 T | 3.23 | 3.66 | 3.39 | 3.93 |
| 1.5 T | 7.41 | 8.088 | 7.47 | 8.84 |

Table 3.7. RELAP5-3D Error in MHD Pressure Drop Magnitude

| Case | RELAP5-3D Vs Experimental (RELAP5-3D Properties) | RELAP5-3D Vs Experimental (Literature Review Properties) | RELAP5-3D Vs Miyazaki (RELAP5-3D Properties) | RELAP5-3D Vs Miyazaki (Literature Review Properties) |
|--------------|--|--|--|--|
| 0.5 T | 15.58 | 7.04 | 3.51 | 10.66 |
| 1.0 T | 10.43 | 10.57 | 7.93 | 14.93 |
| 1.5 T | 18.07 | 24.32 | 8.82 | 15.78 |

Table 3.8. RELAP5-3D Error in Change in MHD Pressure Drop vs Change in Flow Rate

| Case | RELAP5-3D Vs Experimental (RELAP5-3D Properties) | RELAP5-3D Vs Experimental (Literature Review Properties) | RELAP5-3D Vs Miyazaki (RELAP5-3D Properties) | RELAP5-3D Vs Miyazaki (Literature Review Properties) |
|-------|--|---|--|---|
| 0.5 T | 1.53 | 5.49 | 2.94 | 4.27 |
| 1.0 T | 13.35 | 4.83 | 6.74 | 13.84 |
| 1.5 T | 9.15 | 0.85 | 8.41 | 15.46 |

However, in terms of change in pressure drop over change in velocity, the calculations using the literature review properties more closely match the experimental values across all the cases with a maximum relative error of 5.5%. I also see that the data calculated using the RELAP5-3D properties agree more closely with the correlation by Miyazaki with a maximum relative error of 8.41%, which tends to overestimate the MHD pressure drop. With this information, we determine that the MHD implementation is valid and that the PbLi thermophysical properties within the literature review are more appropriate for use in the MHD pressure drop coefficient calculations.

Conclusions

From these studies, we can determine that RELAP5-3D is capable of capturing the thermal-hydraulic behavior of PbLi systems, and is capable of accurately capturing uniform MHD pressure drop phenomena. The representative loop and natural circulation loop ROMs provide baseline validation cases for the heat transfer and pressure phenomena. The heat transfer and pressure drop of the representative loop showed excellent agreement with the analytical calculations and the null transient temperatures and flow rate of the natural circulation loop converged with good agreement to the steady state temperatures. Based on the ALEX benchmark data, the calculations provided by the RELAP5-3D ROM is in good agreement with high fidelity 3-D code predictions of uniform MHD pressure drop. The MaPLE loop validation study proves that the uniform field MHD pressure drop correlation implemented in our ROMs is valid across a variety of magnetic field strengths and flow rates, and should be implemented using the literature reviewed thermophysical properties of PbLi.

CHAPTER FOUR

DCLL MODEL FOR THERMAL-HYDRAULIC ANALYSIS

Model Development and Specifications

In this section, we develop a RELAP5-3D model of the DCLL blanket during a representative startup transient. The channel and flow specifications used for this model are the design values for the inboard blanket of the FNSF system [7, 8, 37]. Each inboard blanket sector within the FNSF, seen in Figure 4.1., is a 22.5 degree slice of the full torus that contains 5 flow channel pairs consisting of one front and one back flow channel. Our model contains one pair of flow channels represented by the nodalization diagram in Figure 4.2. This simplification is made assuming that within a corresponding full sector model, the MHD pressure drop and flow conditions within each flow channel pair should be the same based on the symmetry of the system. A representative 3-D channel cross section is shown in Figure 4.3. The model channel walls are considered to be made of SiC and gap flow is not considered.

The flowrate of the system is calculated as 1/80 the full inboard blanket flow rate accounting for 16 toroidal sectors with 5 channel pairs of equal flow distribution. We assume that the flow within the channels is fully developed flow to satisfy the validated MHD correlations. This is a reasonable assumption since within the ALEX facility experiments, the flow became fully developed within a few centimeters while the total length of the poloidal channels is around 7 meters [84]. Our magnetic field strength within the model is assumed to be uniform following the assumption of a characteristic field strength for the inboard side, 10 T [8]. The electrical conductivity of the SiC flow channel insert is taken from [8] based on the high-temperature inboard blanket requirements and properties of PbLi for the MHD correlation are calculated using the literature review properties as determined in Section 3. A heat structure is attached to both the front and back channels that impose a convective boundary on the channel side and are insulated to the surroundings. The volumetric heat generation within the blanket region is applied as an equivalent heat flux across the convective boundary. To account for the channel being insulated, the heat flux is scaled to assume a 78% retention rate based on a 1-D heat transfer analysis conducted with the inclusion of the structural helium coolant channels [8]. A comprehensive list of operational parameters used in this study are listed in Table 4.1.

The equivalent heat fluxes applied to the PbLi flow channels were determined using the volumetric heat source correlation in Eq. 4. This is based on a model described in [37, 62, 85], for a neutronics analysis of the ITER system using the DANTSYS code.

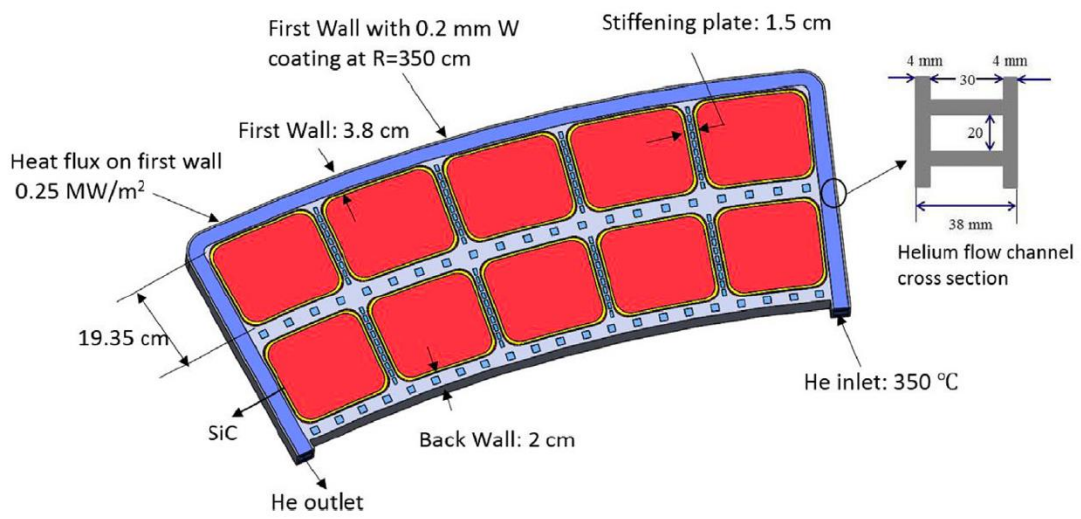


Figure 4.1. FNSF Inboard Blanket Sector Cross Section [7]

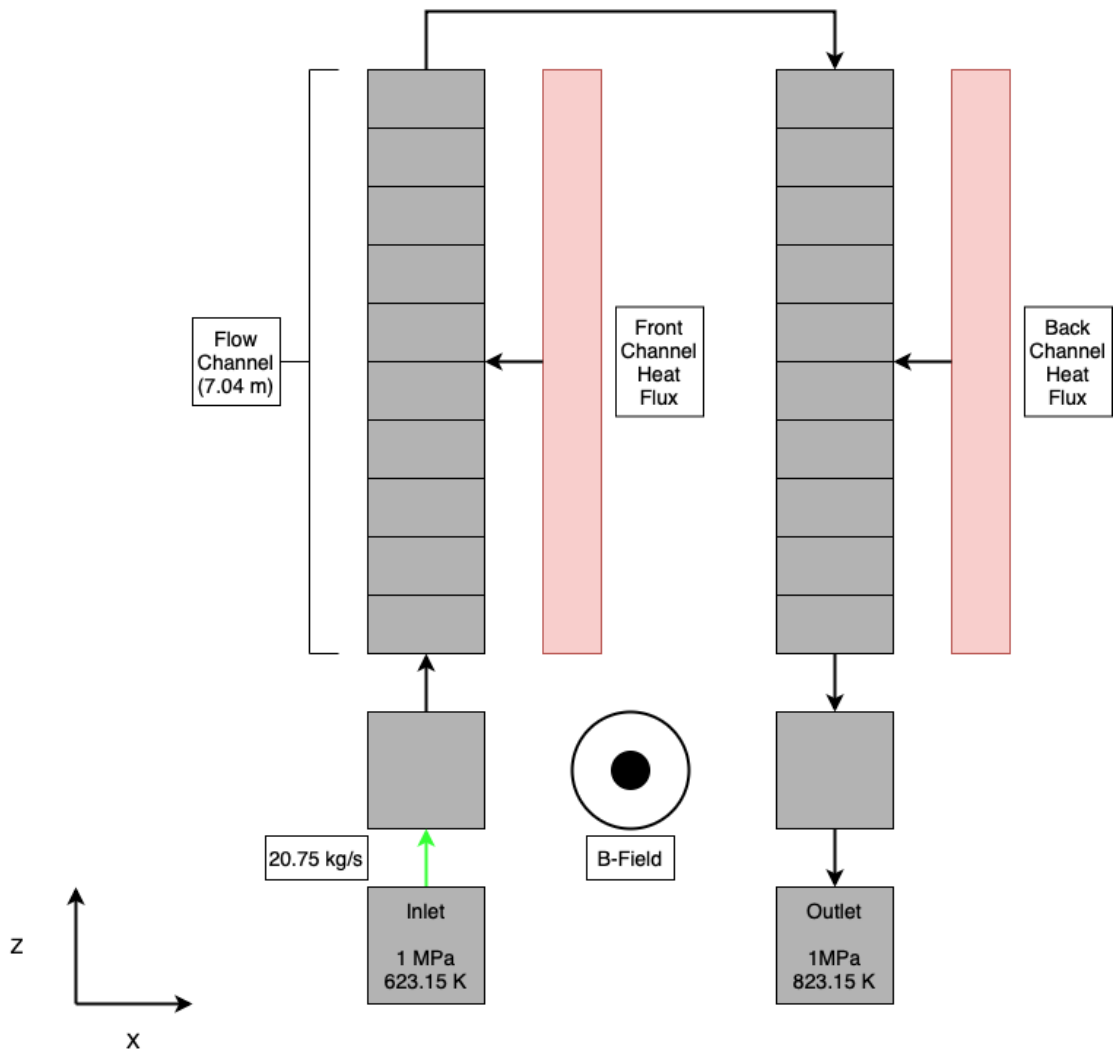


Figure 4.2. DCLL Model Nodalization Diagram

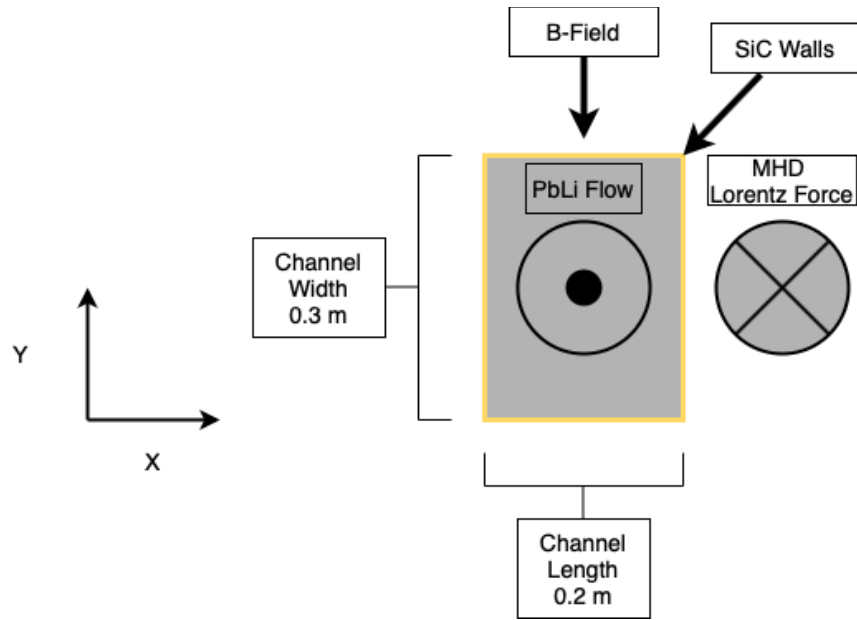


Figure 4.3. Representative DCLL Channel Cross Section

Table 4.1. DCLL Model Operational and MHD Parameters.

| Parameter | | Value | Units |
|------------------------------------|------------|-----------------------|-------------------|
| Inlet Temperature | T | 623.15 | K |
| Channel Radial Width | c | 0.2 | M |
| Channel Toroidal Width | b | 0.3 | M |
| Channel Poloidal Height | h | 7.04 | M |
| FCI Wall Thickness | t_w | 0.005 | M |
| Fluid Electrical Conductivity [74] | σ_f | 8.67×10^5 | 1/ Ω m |
| FCI Electrical Conductivity | σ_w | 1 | 1/ Ω m |
| Fluid Density [74] | ρ_f | 9778 | kg/m ³ |
| Fluid Dynamic Viscosity [74] | μ_f | 1.13×10^{-3} | Pa*s |
| Equivalent Heat Flux (Front) | q''_F | 4.11 | MW/m ² |
| Equivalent Heat Flux (Back) | q''_B | 1.53 | MW/m ² |
| Mass Flow Rate | \dot{m} | 20.75 | kg/s |
| Magnetic Field Strength | B | 10 | T |

Within this relationship, the variable x is the distance from the center of the bulk flow along the radial direction, and the variable c is the channel width in the radial direction. To apply this heat source to the model, the volumetric heat source was converted into an equivalent heat flux by integrating over the radial depth of each channel. This heat flux was normalized to the power of FNSF using a ratio based on the volume of the channels. The dimensions of the channels are approximately the same in the radial and toroidal direction $\sim .2\text{m}$ and $\sim .3\text{m}$, respectively, but the TBM within ITER is only 2m in the poloidal direction [62], as compared to the 7m FNSF channels as described in Table 7. This gave a normalization factor of 3.57 for the blanket heating distribution. As previously mentioned, the model assumed no heat transfer to the surrounding structures and was assumed that only 78% of the volumetric heat stayed within the bulk flow based on a simplified heat transfer analysis from [8]. This volumetric heat source, similar to the blanket flow rate, was also considered to be based on the full inboard blanket and was divided by a factor of 16 . The normalized power density distribution within the channel using the calculated normalization factor and accounting for the heat transfer to helium flow is seen in Figure 4.4.

$$Q = 3 \times 10^7 [e^{-10(x + c/2)}] \quad (4)$$

An initial comparison study between high fidelity CFD calculations on 3-D MHD pressure drop and RELAP5-3D calculations was conducted. The MHD pressure drop calculated by RELAP5-3D was 0.090 MPa which is on the same order of magnitude as the 3-D MHD pressure drop of 0.013 MPa [8]. This is likely the case since our model has a higher velocity, 0.575 m/s in my model to 0.125 m/s in the high fidelity model, and a higher fluid density; 9627 kg/m^3 in my model to 9300 kg/m^3 in the high fidelity model. Based on the trends shown in the validation study, decreasing the flow rate would decrease the MHD pressure drop across the channel. It can be noted that the pressure drop within these simulations is on the same order of magnitude than those from our other benchmarking studies even though the scale of the system and magnetic field strength are much larger. This is attributed to the use of the FCI within the channel. Since the wall electrical conductivity of the SiC FCI is much lower than that of the previous experiments which utilized RAFM steel, the order of magnitude of the MHD pressure drop is significantly reduced. This is consistent with several studies regarding the use of a SiC FCI within the channels of the DCLL design [20, 38-40].

Startup Transient Results

There are currently no experimental startup transients for commercial fusion power plant designs, however tokamak systems have previously performed long lasting plasma pulses on the order of several minutes. Transient analysis was performed using simulation data from Tore Supra program based on its history of high-power, long-term plasma pulses [72].

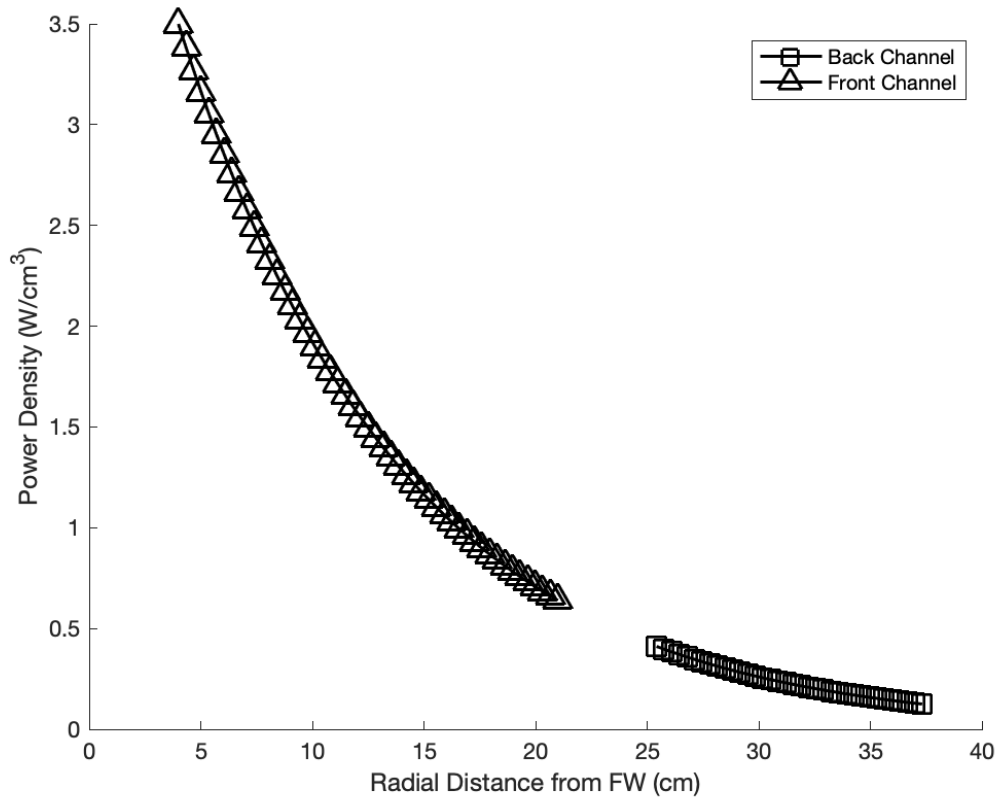


Figure 4.4. DCLL Radial Power Density Distribution

To emulate a startup transient, we used a speculated startup transient accounting for the power ramp limitations of tandem mirror systems as discussed within Section 2. The relative power curve is shown in Figure 4.5 and incorporates a power ramp rate of 5% per minute. The equivalent heat flux to the channel was scaled based on the relative power curve and applied to both the front and back channel. Since the MHD pressure drop at nominal magnetic field strength is a small order of magnitude compared to the elevation pressure drop of about 0.62 MPa, we assumed that the MHD forms loss factor to be constant at its maximum value throughout the transient.

The simulated outlet temperature of the DCLL channel is shown in Figure 4.6. A theoretical calculation of the nominal outlet temperature within the channel using the relationship $Q = \dot{m}C_p\Delta T$ provided a temperature of 820.29K which matched the steady state outlet temperature calculated by the RELAP5-3D, 821.57K. The normalized heating profile from ITER applied to our ROM gives an outlet temperature that nearly matches the design value outlet temperature, 823 K [8]. This analysis can be further improved with heating profiles developed based on a model of the FNSF using a component level neutronics code, and with the addition of thermally coupled helium channels. However, with this developed baseline model, we conclude that the developed model in RELAP5-3D code can accurately calculate the outlet temperature and pressure drop within the DCLL channel under transient conditions.

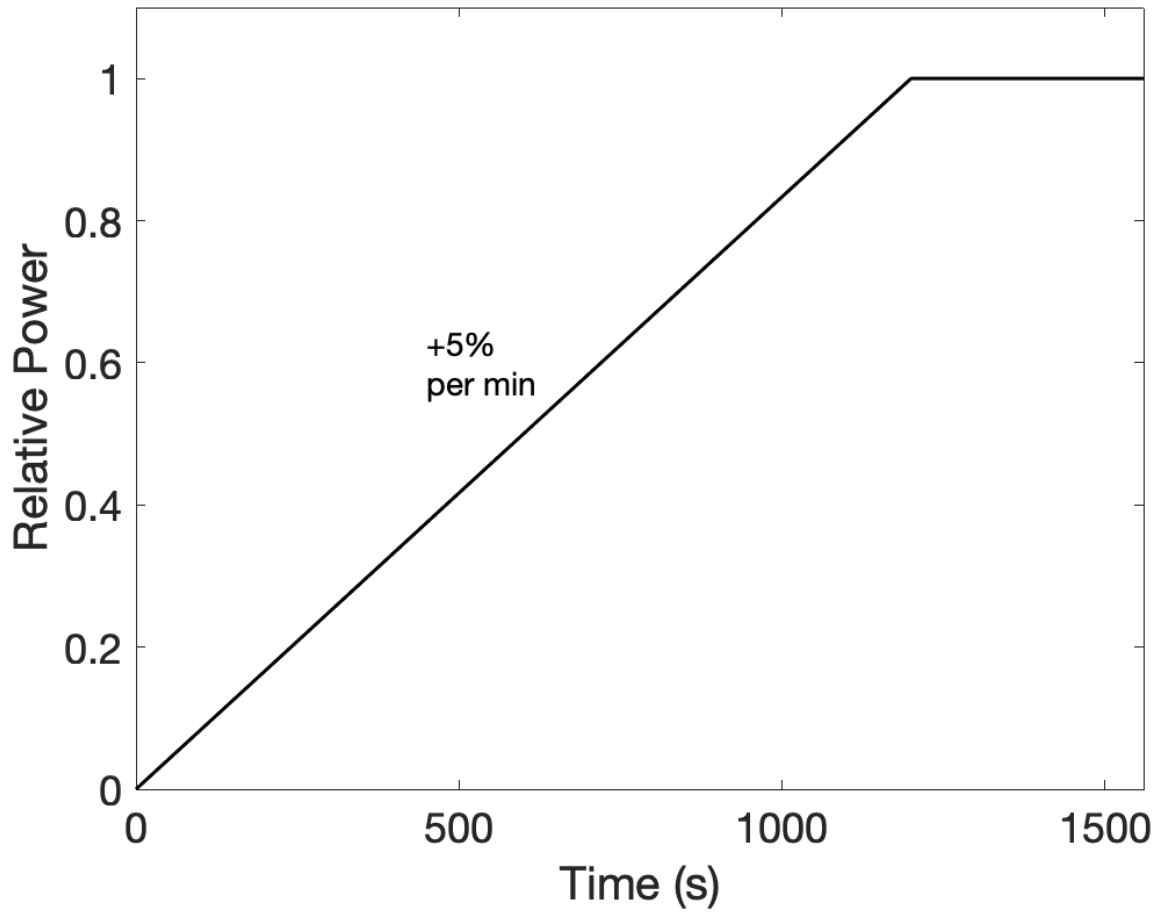


Figure 4.5. DCLL Normalized Representative Startup Transient

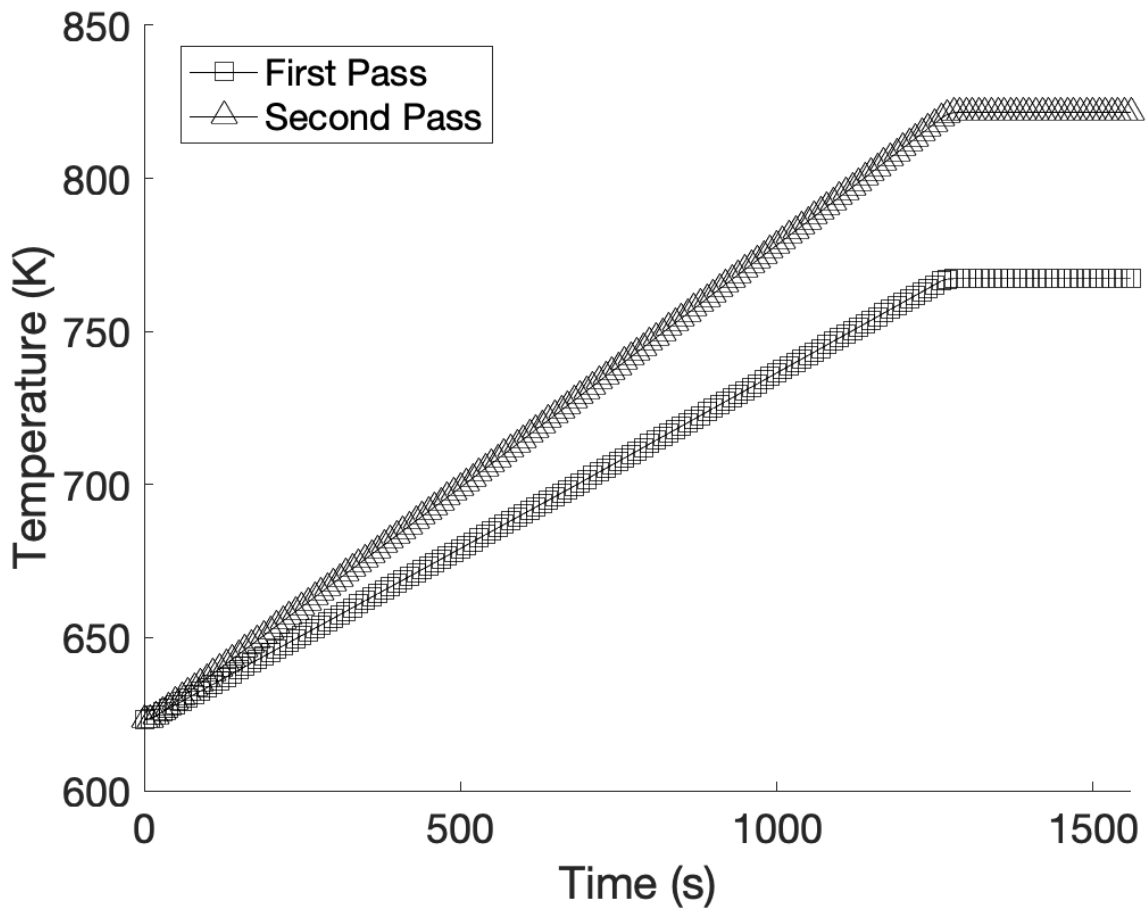


Figure 4.6. DCLL Transient Outlet Temperature

CHAPTER FIVE

CONCLUSIONS AND RECOMMENDATIONS

Within this thesis, I have established an experimental validation basis for the RELAP5-3D code for the analysis of PbLi systems under the effects of a uniform magnetic field. Although the analysis presented is conservative in its assumptions, it provides a baseline model for transient analysis of the DCLL blanket system with good agreement with literature design basis values. There is lots of room for improvement in the current model starting with adding thermally coupled helium flow channels surrounding the current PbLi channel model. Additionally, to reduce the number of assumptions regarding the heating profile, we can implement a profile from a high fidelity neutronics code. For example, by coupling the RELAP5-3D solver to a neutronics code such as MCNP, we could implement heating using a model with the source and material composition data of the FNSF design, rather than the current normalized heating profile from ITER. This would also allow for the capability for iterative calculations of the blanket heat transfer and neutronics at each timestep during the transient if necessary.

At this time, RELAP5-3D is only capable of constant, uniform MHD effects with the implementation demonstrated within this thesis. The capability for uniform and fringing MHD effects was previously implemented in the ATHENA and RELAP5-3D code, but has since been unable to use on the available RELAP5-3D version that was used for this analysis. Further information regarding the formulation of the fringing field and geometric influence were unable to be accessed through the sources available to The University of Tennessee Knoxville. This included the formulation of f_{config} and the tabulated values for the calculation of δ as described in Chapter 3. I believe that in order to truly implement MHD with spatial variation, the RELAP5-3D source code would need to be updated rather than trying to use the equivalent friction factor approach.

Moreover, the current model does not account for the change in the channel flow profile due to the MHD interactions. This means that any potential change in wall velocity will not change the heat transfer within the channel which is not realistic. This is another capability that will need to be implemented within the RELAP5-3D source code in order to be incorporated into future MHD models. With the inclusion of the SiC FCI in this model, the sidewall jets will have a velocity comparable to the bulk flow creating a velocity profile resembling that of fully developed flow [8]. However, this could still be relevant if the corrosion and irradiation of the SiC degrades the insulating properties such as the previously inspected foam SiC FCI [8, 47]. Another inclusion that is required in the future is the inclusion of and thermal coupling of the gap flow region. For the Hartmann walls, this can be accomplished using additional heat structures to model the steel, PbLi and SiC layers as solids since the flowrate within these regions of the channels are practically stagnant, however, since the gap is not insulated, the

non-conducting sidewall gap flow will have high velocity jets and must be modeled as flowing liquid [8].

The main difficulties surrounding the accurate simulation of MHD flow is the lack of methods that can handle complex flow geometries such as manifolds that exist within fusion blanket systems [49]. A recent study confirmed that RELAP5/MOD3.3, a variant of RELAP as described in Chapter 1, was capable of capturing 3-D MHD pressure effects with good agreement to experimental results. This is significant since if this version of RELAP is capable of 1-D analysis similar to that presented within this thesis, but with the capabilities of fringing field and varying channel geometry as demonstrated in the 3-D analysis, it could be a great tool for code-to-code comparison studies for verifying pressure drop calculations of MHD pressure drops within RELAP5-3D. Alternatively, these calculation methods could also be implemented within RELAP5-3D directly.

Future work on this model also includes developing a simple thermomechanical analysis to determine the limiting rate of power increase during operation. The current startup transient is based on light water thermal expansion limits rather than PbLi thermal expansion. By developing a simple thermomechanical analysis, future design choices can be guided toward either regulating the plasma power or improving the components that would overcome this rapid increase in power as outlined in the tandem mirror analysis [67]. In this case, the main consideration would be the stability of the plasma during the startup transient. If the plasma is not stable at each power level during the transient, the blanket would require either increasingly more pre-heating of the coolant channels or faster pump response time. This would be necessary to account for the potential rapid increase in plasma power as demonstrated within the Tore Supra transient.

Currently, I have developed an initial model for implementing several of these suggested changes. The new model implements heating profiles generated using a high fidelity MCNP model. The model consists of one sector of the FNSF with a source that is scaled to the power of the plasma and reflective boundary conditions. A CAD diagram of the model sector and the FNSF system is shown in Figure 5.1 [35]. The heating profiles are shown in Figure 5.2, and are azimuthally averaged over the sector. The axial variations of the heating profiles are shown from the midplane at $z = 386.1$ to just above the reflector at $z = 175.5$ cm. The heating at the midplane was applied to the full length of the channel as a conservative estimate. The helium channels in the DCLL design consists of many toroidal passes across the sector with a final pass through the center [7]. This was implemented as several channels of equivalent volume and flow velocity thermally coupled the PbLi channels. A diagram of the helium channel coupling is shown in Figure 5.3.

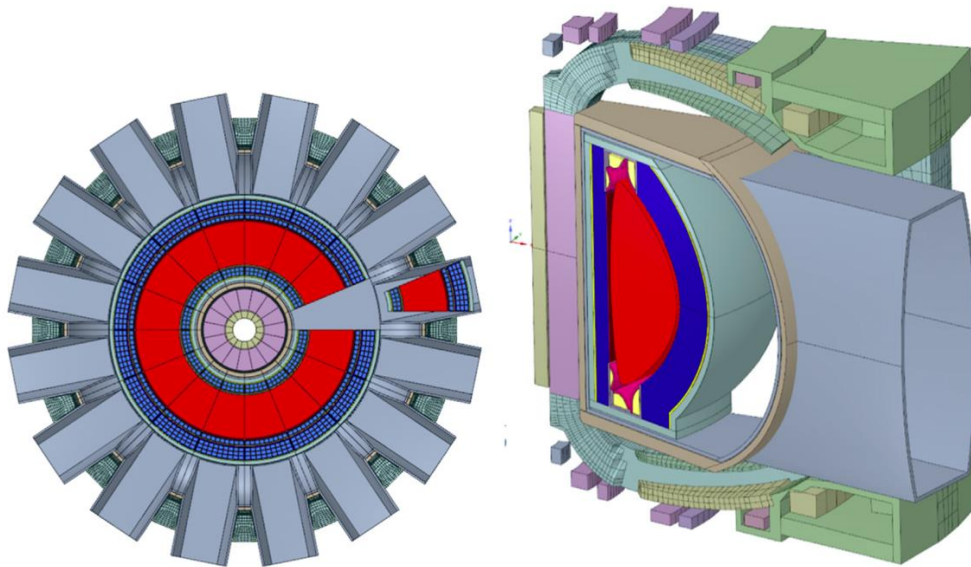


Figure 5.1. MCNP CAD Model Diagram of the FNSF (Left) and of One Sector (Right)

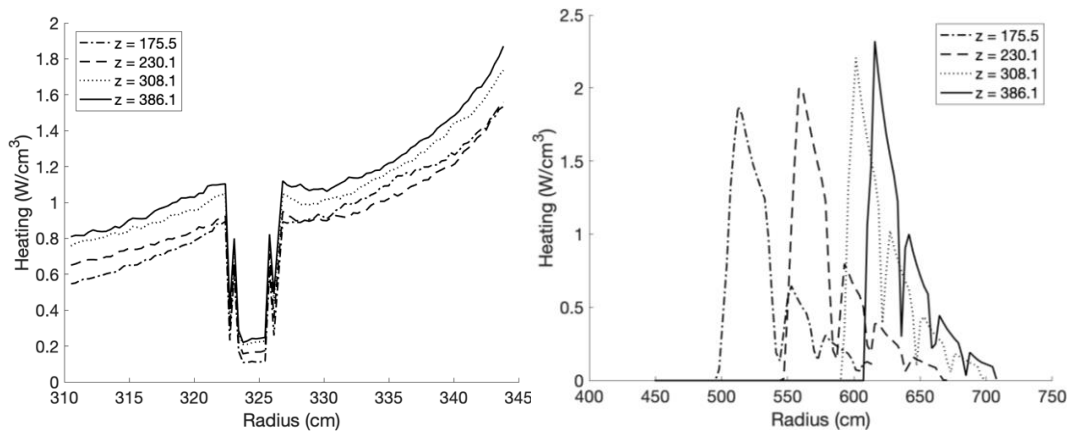


Figure 5.2. MCNP Calculated Radial Heating Profiles for the Inboard Blanket (Left) and Outboard Blanket (Right)

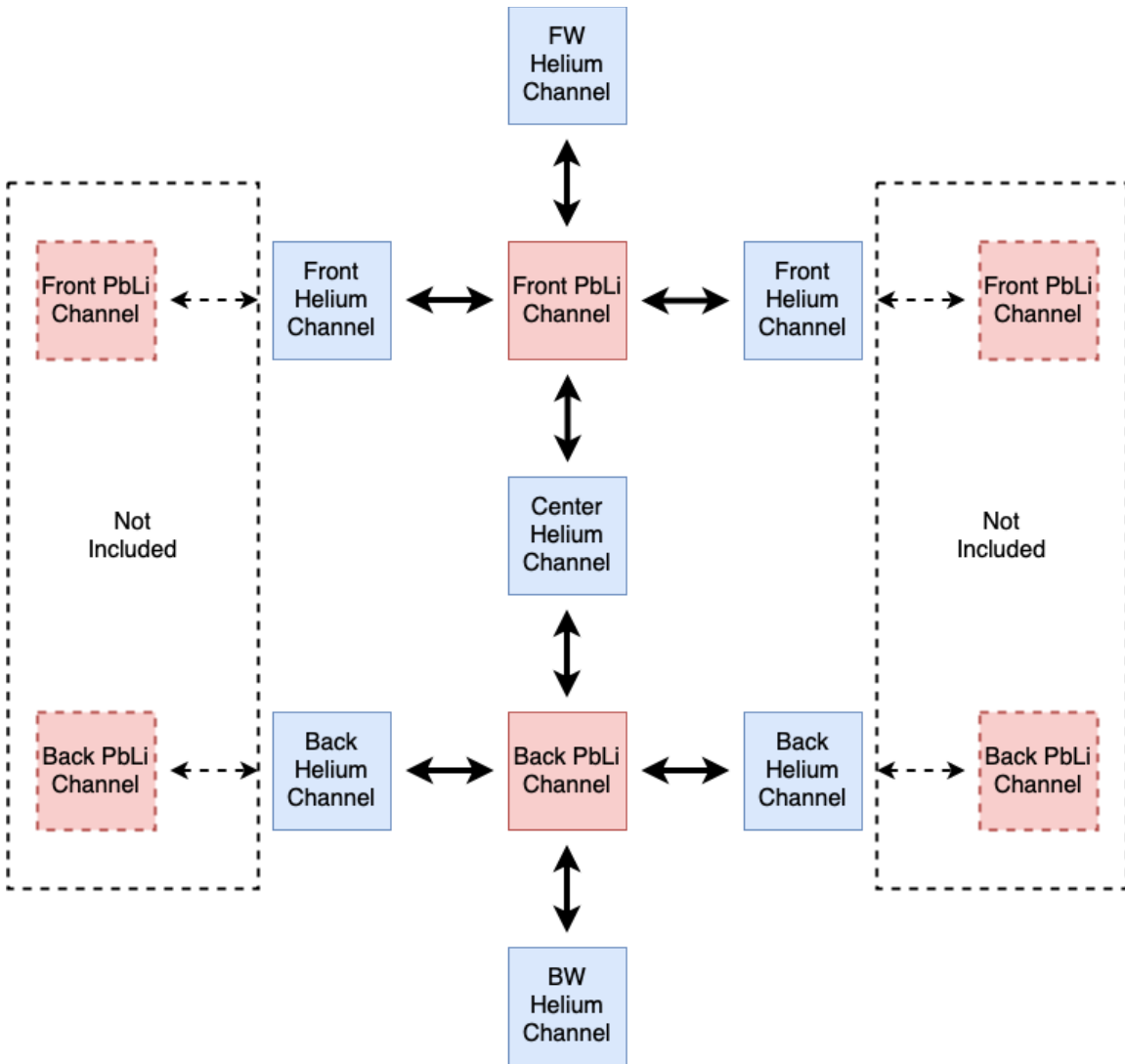


Figure 5.3. RELAP5-3D DCLL Blanket Helium Channel Coupling Diagram

The startup transient conducted for this model is based on speculated tandem mirror transients that incorporate steady state operation at 20%, 50%, and 80% full power to perform tests on specific reactor systems over the course of a day [67]. The transient outlet temperatures of both the PbLi and helium channels are shown in Figures 5.4 and 5.5. A comparison of the analytically predicted temperature, RELAP5-3D calculated temperature, and design value temperatures is shown in Table 5.1. The PbLi outlet temperatures match within 5K of the design values but the average helium outlet temperature is around half the design value. This is likely due to the model implementing the helium channels as one pass rather than two passes as shown in the literature, and since the first wall heat flux is not implemented. Further modeling improvements would include changing the helium channel coupling to incorporate two passes, and all previous changes mentioned.

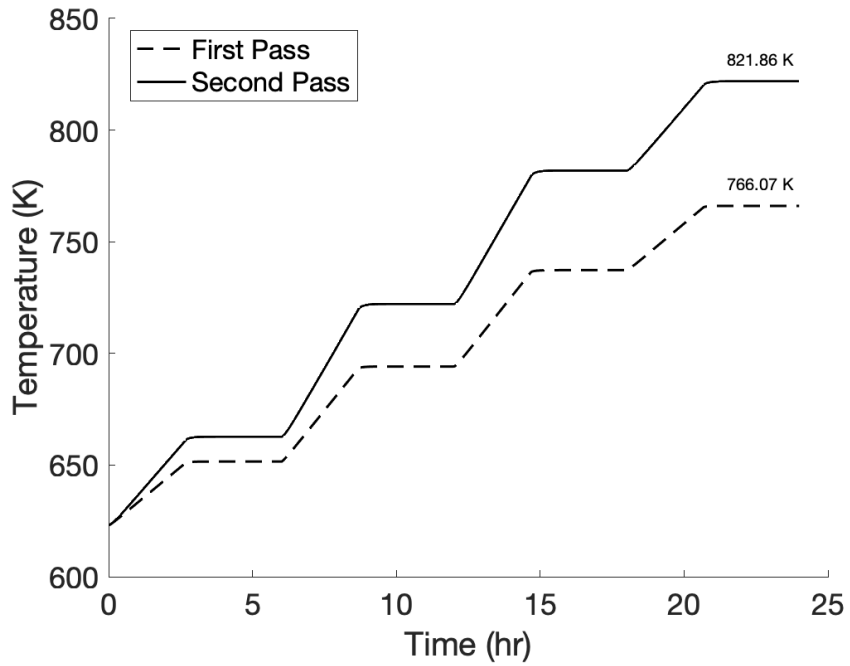


Figure 5.4. DCLL Transient PbLi Outlet Temperature

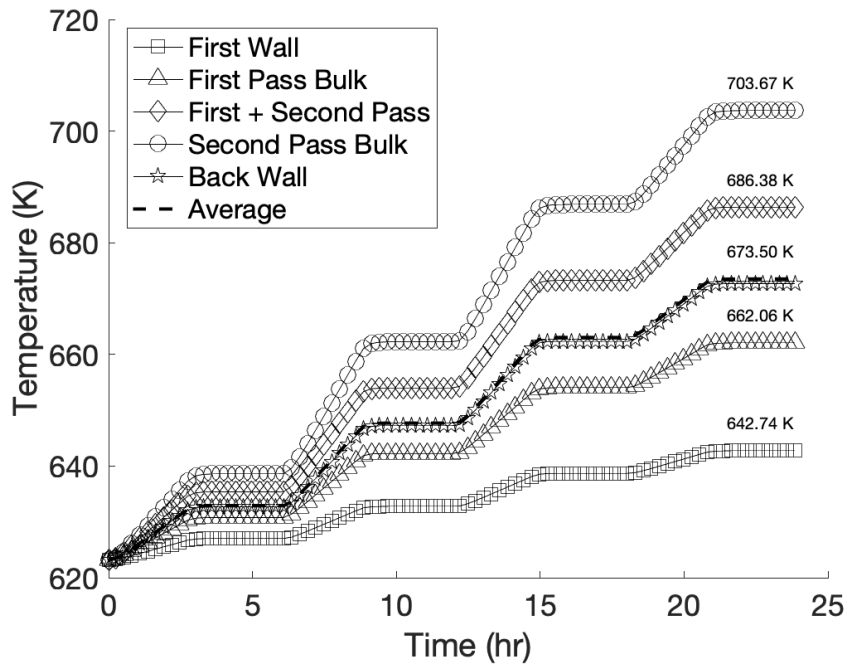


Figure 5.5. DCLL Transient Helium Outlet Temperature

Table 5.1. DCLL Blanket Outlet Temperature with Helium Coupling

| Calculation | PbLi Outlet Temperature (K) | He Outlet Temperature (K) |
|---------------------|------------------------------------|----------------------------------|
| Predicted | 834.89 | N/a |
| RELAP5-3D | 821.86 | 673.50 |
| Design Value | 823.15 | 748.15 |

LIST OF REFERENCES

- [1] D. Meade, 50 years of fusion research, *Nuclear fusion* 50(1) (2010) 014004.
- [2] C.E. Kessel, J.P. Blanchard, A. Davis, L. El-Guebaly, N. Ghoniem, P.W. Humrickhouse, S. Malang, B.J. Merrill, N.B. Morley, G.H. Neilson, M.E. Rensink, T.D. Rognlien, A.F. Rowcliffe, S. Smolentsev, L.L. Snead, M.S. Tillack, P. Titus, L.M. Waganer, A. Ying, K. Young, Y. Zhai, The Fusion Nuclear Science Facility, the Critical Step in the Pathway to Fusion Energy, *Fusion science and technology* 68(2) (2015) 225-236.
- [3] S. Malang, M. Tillack, C.P.C. Wong, N. Morley, S. Smolentsev, Development of the Lead Lithium (DCLL) Blanket Concept, *Fusion Science and Technology* 60(1) (2011) 249-256.
- [4] C. Soto, S. Smolentsev, C. García-Rosales, Mitigation of MHD phenomena in DCLL blankets by Flow Channel Inserts based on a SiC-sandwich material concept, *Fusion Engineering and Design* 151 (2020) 111381.
- [5] S.B. Seo, R. Hernandez, M. O'Neal, N. Meehan, F.S. Novais, M. Rizk, G.I. Maldonado, N.R. Brown, A review of thermal hydraulics systems analysis for breeding blanket design and future needs for fusion engineering demonstration facility design and licensing, *Fusion Engineering and Design* 172 (2021) 112769.
- [6] M. Abdou, N.B. Morley, S. Smolentsev, A. Ying, S. Malang, A. Rowcliffe, M. Ulrickson, Blanket/first wall challenges and required R&D on the pathway to DEMO, *Fusion engineering and design* 100(C) (2015) 2-43.
- [7] Y. Huang, M.S. Tillack, N.M. Ghoniem, J.P. Blanchard, L.A. El-Guebaly, C.E. Kessel, Multiphysics modeling of the FW/Blanket of the U.S. fusion nuclear science facility (FNSF), *Fusion Engineering and Design* 135 (2018) 279-289.
- [8] S. Smolentsev, T. Rhodes, G. Pulugundla, C. Courtessole, M. Abdou, S. Malang, M. Tillack, C. Kessel, MHD thermohydraulics analysis and supporting R&D for DCLL blanket in the FNSF, *Fusion engineering and design* 135(PB) (2018) 314-323.
- [9] A. Davis, M. Harb, L. El-Guebaly, P. Wilson, E. Marriott, Neutronics aspects of the FESS-FNSF, *Fusion Engineering and Design* 135 (2018) 271-278.
- [10] RELAP5-3D, Idaho National Engineering and Environmental Laboratory RELAP5-3D/GWJ/10/27/2015 (2015).
- [11] M.-Y. Ahn, S. Cho, D.H. Kim, E.-S. Lee, H.-S. Kim, J.-S. Suh, S. Yun, N.Z. Cho, Preliminary safety analysis of Korea Helium Cooled Solid Breeder Test Blanket Module, *Fusion engineering and design* 83(10) (2008) 1753-1758.

- [12] L. Melchiorri, V. Narcisi, F. Giannetti, G. Caruso, A. Tassone, Development of a RELAP5/MOD3.3 Module for MHD Pressure Drop Analysis in Liquid Metals Loops: Verification and Validation, *Energies* 14(17) (2021).
- [13] M. Nakamura, K. Tobita, Y. Someya, H. Utoh, Y. Sakamoto, W. Gulden, Thermohydraulic responses of a water-cooled tokamak fusion DEMO to loss-of-coolant accidents, *Nuclear fusion* 55(12) (2015) 123008.
- [14] X.Z. Jin, BB LOCA analysis for the reference design of the EU DEMO HCPB blanket concept, *Fusion engineering and design* 136 (2018) 958-963.
- [15] M. D'Onorio, F. Giannetti, M.T. Porfiri, G. Caruso, Preliminary safety analysis of an in-vessel LOCA for the EU-DEMO WCLL blanket concept, *Fusion engineering and design* 155 (2020) 111560.
- [16] A. Zappatore, A. Froio, G.A. Spagnuolo, R. Zanino, 3D transient CFD simulation of an in-vessel loss-of-coolant accident in the EU DEMO fusion reactor, *Nuclear fusion* 60(12) (2020).
- [17] H. Wang, W. Wang, Y. Bai, H. Chen, Preliminary thermal-hydraulics design of the dual-cooled lithium lead blanket for FDS-II, *Fusion engineering and design* 75 (2005) 841-845.
- [18] I. Lupelli, A. Malizia, M. Richetta, L.A. Poggi, J.F. Ciparisse, M. Gelfusa, P. Gaudio, Simulations and Experiments to Reach Numerical Multiphase Informations for Security Analysis on Large Volume Vacuum Systems Like Tokamaks, *Journal of fusion energy* 34(5) (2015) 959-978.
- [19] A. Malizia, L. Poggi, J.-F. Ciparisse, R. Rossi, C. Bellecci, P. Gaudio, A Review of Dangerous Dust in Fusion Reactors: from Its Creation to Its Resuspension in Case of LOCA and LOVA, *Energies (Basel)* 9(8) (2016) 578.
- [20] F.R. Ugorri, S. Smolentsev, I. Fernández-Berceruelo, D. Rapisarda, I. Palermo, A. Ibarra, Magnetohydrodynamic and thermal analysis of PbLi flows in poloidal channels with flow channel insert for the EU-DCLL blanket, *Nuclear fusion* 58(10) (2018) 106001.
- [21] A. Froio, A. Bertinetti, L. Savoldi, R. Zanino, F. Cismondi, S. Ciattaglia, Benchmark of the GETTHEM Vacuum Vessel Pressure Suppression System (VVPSS) model for a helium-cooled EU DEMO blanket, 2017.
- [22] A. Froio, A. Bertinetti, S. Ciattaglia, F. Cismondi, L. Savoldi, R. Zanino, Modelling an in-vessel loss of coolant accident in the EU DEMO WCLL breeding blanket with the GETTHEM code, *Fusion engineering and design* 136 (2018) 1226-1230.

- [23] A. Froio, L. Barucca, S. Ciattaglia, F. Cismondi, L. Savoldi, R. Zanino, Analysis of the effects of primary heat transfer system isolation valves in case of in-vessel loss-of-coolant accidents in the EU DEMO, Fusion engineering and design 159 (2020) 111926.
- [24] S. Smolentsev, N. Morley, M. Abdou, Code development for analysis of MHD pressure drop reduction in a liquid metal blanket using insulation technique based on a fully developed flow model, Fusion Engineering and Design 73(1) (2005) 83-93.
- [25] T. Marshall, M.T. Porfiri, L. Topilski, B. Merrill, Fusion safety codes: international modeling with MELCOR and ATHENA-INTRA, Fusion Engineering and Design 63-64 (2002) 243-249.
- [26] D. Panayotov, Y. Poitevin, A. Grief, M. Trow, M. Dillistone, J.T. Murgatroyd, S. Owen, K. Peers, A. Lyons, A. Heaton, R. Scott, B.J. Merrill, P. Humrickhouse, A Methodology for Accident Analysis of Fusion Breeder Blankets and Its Application to Helium-Cooled Lead-Lithium Blanket, IEEE Transactions on Plasma Science 44(10) (2016) 2511-2522.
- [27] D. Panayotov, A. Grief, B.J. Merrill, P. Humrickhouse, M. Trow, M. Dillistone, J.T. Murgatroyd, S. Owen, Y. Poitevin, K. Peers, A. Lyons, A. Heaton, R. Scott, Methodology for accident analyses of fusion breeder blankets and its application to helium-cooled pebble bed blanket, Fusion engineering and design 109-111 (2016) 1574-1580.
- [28] J. Murgatroyd, S. Owen, A. Grief, D. Panayotov, C. Saunders, Qualification of MELCOR and RELAP5 models for EU HCPB TBS accident analyses, Fusion Engineering and Design 124 (2017) 1251-1256.
- [29] A. Grief, S. Owen, J. Murgatroyd, D. Panayotov, B. Merrill, P. Humrickhouse, C. Saunders, Qualification of MELCOR and RELAP5 models for EU HCLL TBS accident analyses, Fusion Engineering and Design 124 (2017) 1165-1170.
- [30] B.W. D. Prelewicz, C. Delfino, COMMERCIAL GRADE DEDICATION OF RELAP5-3D, NURETH-16, Chicago, IL, USA, 2015.
- [31] RELAP5-3D Code Manual, (INL/MIS-15-36723, Idaho National Laboratory, Idaho Falls, Idaho 83415, Revision 4.4) (2018).
- [32] R.A. Riemke, C.B. Davis, R.R. Schultz, RELAP5-3D Code Includes ATHENA Features and Models, 14th International Conference on Nuclear Engineering, 2006, pp. 209-217.

- [33] B.J. Merrill, P.W. Humrickhouse, S.J. Yoon, Modifications to the MELCOR-TMAP code to simultaneously treat multiple fusion coolants, *Fusion Engineering and Design* 146 (2018).
- [34] N. Brown, S. Seo, *Safety of Nuclear Reactors*, 2021.
- [35] C.E. Kessel, J.P. Blanchard, A. Davis, L. El-Guebaly, L.M. Garrison, N.M. Ghoniem, P.W. Humrickhouse, Y. Huang, Y. Kato, A. Khodak, E.P. Marriott, S. Malang, N.B. Morley, G.H. Neilson, J. Rapp, M.E. Rensink, T.D. Rognlien, A.F. Rowcliffe, S. Smolentsev, L.L. Snead, M.S. Tillack, P. Titus, L.M. Waganer, G.M. Wallace, S.J. Wukitch, A. Ying, K. Young, Y. Zhai, Overview of the fusion nuclear science facility, a credible break-in step on the path to fusion energy, *Fusion Engineering and Design* 135 (2018) 236-270.
- [36] L. Bühler, T. Arlt, T. Boeck, L. Braidon, V. Chowdhury, D. Krasnov, C. Mistrangelo, S. Molokov, J. Priede, Magnetically induced instabilities in duct flows, *IOP Conference Series: Materials Science and Engineering* 228 (2017) 012003.
- [37] S. Smolentsev, M. Abdou, N.B. Morley, M. Sawan, S. Malang, C. Wong, Numerical analysis of MHD flow and heat transfer in a poloidal channel of the DCLL blanket with a SiCf/SiC flow channel insert, *Fusion engineering and design* 81(1-7) (2006) 549-553.
- [38] C. Soto, C. García-Rosales, J. Echeberria, J.M. Martínez-Esnaola, T. Hernández, M. Malo, E. Platacis, F. Muktepavela, SiC-based sandwich material for Flow Channel Inserts in DCLL blankets: Manufacturing, characterization, corrosion tests, *Fusion engineering and design* 124 (2017) 958-963.
- [39] C. Soto, J.M. Martínez-Esnaola, C. García-Rosales, Thermomechanical analysis of a Flow Channel Insert based on a SiC-sandwich material concept, *Nuclear materials and energy* 7 (2016) 5-11.
- [40] X. Zhang, Z. Xu, C. Pan, Numerical analysis of MHD duct flow with a flow channel insert, *Fusion Engineering and Design* 85(10) (2010) 2090-2094.
- [41] W.K. Hussam, M.C. Thompson, G.J. Sheard, Dynamics and heat transfer in a quasi-two-dimensional MHD flow past a circular cylinder in a duct at high Hartmann number, *International Journal of Heat and Mass Transfer* 54(5) (2011) 1091-1100.
- [42] L.M. Giancarli, M. Abdou, D.J. Campbell, V.A. Chuyanov, M.Y. Ahn, M. Enoeda, C. Pan, Y. Poitevin, E. Rajendra Kumar, I. Ricapito, Y. Strebkov, S. Suzuki, P.C. Wong, M. Zmitko, Overview of the ITER TBM Program, *Fusion Engineering and Design* 87(5) (2012) 395-402.

- [43] C.B. Reed, B.F. Picologlou, P.V. Dauzvardis, Experimental Facility for Studying MHD Effects in Liquid Metal Cooled Blankets, *Fusion Technology* 8(1P2A) (1985) 257-263.
- [44] S. Smolentsev, F.C. Li, N. Morley, Y. Ueki, M. Abdou, T. Sketchley, Construction and initial operation of MHD PbLi facility at UCLA, *Fusion Engineering and Design* 88(5) (2013) 317-326.
- [45] T.Q. Hua, J.S. Walker, B.F. Picologlou, C.B. Reed, Three-dimensional MHD (magnetohydrodynamic) flows in rectangular ducts of liquid-metal-cooled blankets, United States, 1988.
- [46] F.C. Li, D. Sutevski, S. Smolentsev, M. Abdou, Experimental and numerical studies of pressure drop in PbLi flows in a circular duct under non-uniform transverse magnetic field, *Fusion Engineering and Design* 88(11) (2013) 3060-3071.
- [47] S. Smolentsev, C. Courtessole, M. Abdou, S. Sharafat, S. Sahu, T. Sketchley, Numerical modeling of first experiments on PbLi MHD flows in a rectangular duct with foam-based SiC flow channel insert, *Fusion Engineering and Design* 108 (2016) 7-20.
- [48] S. Smolentsev, S. Badia, R. Bhattacharyay, L. Bühler, L. Chen, Q. Huang, H.G. Jin, D. Krasnov, D.W. Lee, E.M. de les Valls, C. Mistrangelo, R. Munipalli, M.J. Ni, D. Pashkevich, A. Patel, G. Pulugundla, P. Satyamurthy, A. Snegirev, V. Sviridov, P. Swain, T. Zhou, O. Zikanov, An approach to verification and validation of MHD codes for fusion applications, *Fusion engineering and design* 100 (2015) 65-72.
- [49] C.B. Reed, B.F. Picologlou, T.Q. Hua, J.S. Walker, ALEX results: A comparison of measurements from a round and a rectangular duct with 3-D code predictions, United States, 1987, p. 5.
- [50] J. Feng, H. Chen, Q. He, M. Ye, Further validation of liquid metal MHD code for unstructured grid based on OpenFOAM, *Fusion Engineering and Design* 100 (2015) 260-264.
- [51] C. Alberghi, L. Candido, R. Testoni, M. Utili, M. Zucchetti, Verification and Validation of COMSOL Magnetohydrodynamic Models for Liquid Metal Breeding Blankets Technologies, *Energies* 14(17) (2021).
- [52] N.L. Gajbhiye, P. Throvaunta, V. Eswaran, Validation and verification of a robust 3-D MHD code, *Fusion Engineering and Design* 128 (2018) 7-22.

- [53] M.-J. Ni, R. Munipalli, N. Morley, P. Huang, M. Abdou, Validation Case Results for 2D and 3D MHD Simulations, *Fusion Science and Technology* 52 (2007).
- [54] P.A. Roth, Assessment of the MHD Capability in the ATHENA Code Using Data from the ALEX Facility, *Fusion Technology* 15(2P2B) (1989) 1003-1007.
- [55] J.E. Tolli, Athena MHD Model, EGG-SC-93-107 (1993).
- [56] C.B. Reed, R.C. Haglund, M.E. Miller, Summary report for ITER task - T68: MHD facility preparation for Li/V blanket option, 1995.
- [57] C.B. Reed, R.C. Haglund, M.E. Miller, J.R. Nasiatka, I.R. Kirillov, A.P. Ogorodnikov, G.V. Preslitski, G.P. Goloubovitch, Z.Y. Xu, The Conversion of a Room Temperature NaK Loop to a High Temperature MHD Facility for LI/V Blanket Testing, *Fusion Technology* 30(3P2A) (1996) 1036-1041.
- [58] C.B. Reed, K. Natesan, T.Q. Hua, I.R. Kirillov, I.V. Vitkovski, A.M. Anisimov, Experimental and theoretical MHD performance of a round pipe with an NaK-compatible Al₂O₃ coating, *Fusion Engineering and Design* 27 (1995) 614-626.
- [59] S. Smolentsev, M. Abdou, C. Courtessole, G. Pulugundla, F.C. Li, N. Morley, R. Munipalli, P. Huang, C. Kaczynski, J. Young, T. Rhodes, Y. Yan, REVIEW OF RECENT MHD ACTIVITIES FOR LIQUID METAL BLANKETS IN THE US, *Magnetohydrodynamics (0024-998X)* 53(2) (2017) 411-422.
- [60] R. Munipalli, S. Shankar, M. Ni, N. Morley, Development of a 3-D incompressible free surface MHD computational environment for arbitrary geometries: HIMAG, DOE SBIR phase-ii final report (2003).
- [61] K. Miyazaki, S. Kotake, N. Yamaoka, S. Inoue, Y. Fujii-E, MHD Pressure Drop of NaK Flow in Stainless Steel Pipe, *Nuclear Technology - Fusion* 4(2P2) (1983) 447-452.
- [62] L. Chen, M. Li, M. Ni, N. Zhang, MHD effects and heat transfer analysis in magneto-thermo-fluid-structure coupled field in DCLL blanket, *International Communications in Heat and Mass Transfer* 84 (2017) 110-120.
- [63] NUREG-0800, "Standard Review Plan for the Review of Safety Analysis Reports for Nuclear Power Plants, LWR Edition.", U.S. Nuclear Regulatory Commission (US NRC) (2007).
- [64] the westinghouse pressurized water reactor nuclear power plant, Westinghouse Electric Corporation Water Reactor Divisions (1984).

- [65] N. Ghoniem, K. Taghavi, J.P. Blanchard, S. Grotz, Limits on transient power variations during startup and shutdown of Li-Pb cooled TMR blankets, *Fusion Science and Technology* 4 (1983) 769-774.
- [66] K. Taghavi, N. Ghoniem, Transient thermal-hydraulics considerations of tandem mirror LiPb cooled blankets during start-up/shutdown operations, *Nuclear Engineering and Design. Fusion* 1 (1984) 369-374.
- [67] R.W. Conn, N.M. Ghoniem, S.P. Grotz, F. Najmabadi, K. Taghavi, M.Z. Youssef, Influence of Startup, Shutdown and Staged Power Operation on Tandem Mirror Reactor Design, *Nuclear Technology - Fusion* 4(2P2) (1983) 615-622.
- [68] K. Taghavi, N.M. Ghoniem, Primary loop conditioning and design constraints of Li-Pb cooled tandem mirror reactors during start-up/shutdown operations, *Nuclear Engineering and Design. Fusion* 1(4) (1984) 375-386.
- [69] P.W. Humrickhouse, B.J. Merrill, S.-J. Yoon, L.C. Cadwallader, The Impacts of Liquid Metal Plasma-Facing Components on Fusion Reactor Safety and Tritium Management, *Fusion Science and Technology* 75(8) (2019) 973-1001.
- [70] T. Hoang, C. Bourdelle, X. Garbet, B. Pegourie, J.F. Artaud, V. Basiuk, J. Bucalossi, C. FenziBonizec, F. Clairet, L.-G. Eriksson, C. Gil, R. Guirlet, F. Imbeaux, J. Lasalle, C. Lowry, B. Schunke, J.L. Ségui, J.-M. Travere, E. Tsitrone, L. Vermare, Turbulent particle transport in Tore Supra, *Nuclear Fusion* 46 (2006) 306.
- [71] J. Jacquinet, Steady-state operation of tokamaks: Key physics and technology developments on Tore Supra, International Atomic Energy Agency (IAEA), 2004, p. 3.
- [72] G.M.f.t.T.-S. Team, Overview of steady-state operation on the Tore-Supra tokamak, *Nuclear Fusion* 43(9) (2003) 817-821.
- [73] P.W. Humrickhouse, B.J. Merrill, An equation of state for liquid Pb83Li17, *Fusion engineering and design* 127(C) (2018) 10-16.
- [74] D. Martelli, A. Venturini, M. Utili, Literature review of lead-lithium thermophysical properties, *Fusion Engineering and Design* 138 (2019) 183-195.
- [75] Y. Jiang, S. Smolentsev, J. Jun, B. Pint, C. Kessel, Prediction of PbLi fluid flow and temperature field in a thermal convection loop for qualification of fusion materials, *International journal of heat and mass transfer* 172 (2021) 121198.
- [76] S.J. Pawel, K.A. Unocic, Compatibility of an FeCrAl alloy with flowing Pb-Li in a thermal convection loop, *Journal of Nuclear Materials* 492 (2017) 41-51.

- [77] J. Jun, K.A. Unocic, M.J. Lance, H.M. Meyer, B.A. Pint, Compatibility of FeCrAlMo with flowing PbLi at 500°-650 °C, *Journal of Nuclear Materials* 528 (2020) 151847.
- [78] C. Courtessole, S. Smolentsev, T. Sketchley, M. Abdou, MHD PbLi experiments in MaPLE loop at UCLA, *Fusion Engineering and Design* 109-111 (2016) 1016-1021.
- [79] R.S. Graves, T.G. Kollie, D.L. McElroy, K.E. Gilchrist, The thermal conductivity of AISI 304L stainless steel, *International Journal of Thermophysics* 12(2) (1991) 409-415.
- [80] P.D.A.S.f.M. Harvey, *Engineering properties of steel*, American Society for Metals, Metals Park, Ohio, 1982.
- [81] D.B.I.M. Peckner, *Handbook of stainless steels*, McGraw-Hill, S.L., 1977.
- [82] H.E.G.T.L.A.S.f.M. Boyer, *Metals handbook. Volume 17*, Volume 17, ASM International, [Metals Park, Ohio], 1989.
- [83] A.S.f.M.I.H.C. American Society for Metals, *Metals handbook. V. I V. I*, American Society for Metals, Metals Park, Ohio, 1990.
- [84] B.F. Picologlou, C.B. Reed, T.Q. Hua, A.S. Lavine, The Design of a Heat Transfer Liquid Metal MHD Experiment for ALEX, *Fusion Technology* 15(2P2B) (1989) 1186-1191.
- [85] H. Huang, S. Yin, G. Zhu, Heat transfer performance for DCLL blanket with no-wetting insulator walls, *Theoretical and Applied Mechanics Letters* 9 (2019) 195-201.

VITA

Nicholas A. Meehan graduated from North Carolina State University with a Bachelor of Science in Nuclear Engineering in May of 2020. In the summer of 2020, he began research at the University of Tennessee, Knoxville. Nicholas has presented this work at the American Nuclear Society Annual Meeting virtually in 2021, the Inertial Fusion Energy Science & Technology Community Strategic Planning Workshop in 2022, and at NURETH 19 in 2022. He anticipates to graduate with a Master of Science in Nuclear Engineering in May 2022.